# How the lability of particulate organic matter responded to physical constraints during summer in the Ross Sea

Cristina Misic[1], Anabella Covazzi Harriague[1], Olga Mangoni [2],

Yuri Cotroneo[3], Giuseppe Aulicino[3], Pasquale Castagno[3]

[1] Dipartimento di Scienze della Terra, dell'Ambiente e della Vita – University of Genova, C.so Europa 26, 16132 Genova, Italy

[2] Dipartimento di Biologia, University of Napoli Federico II, Via Mezzocannone, 8, 80134 Napoli, Italy.

[3] Dipartimento di Scienze e Tecnologie, University of Napoli Parthenope, Centro Direzionale di Napoli IS. C4, 80143 Napoli, Italy

Corresponding author:

Cristina Misic,

Dipartimento di Scienze della Terra, dell'Ambiente e della Vita - University of Genova

C.so Europa 26, 16132 Genova, Italy.

Phone: +3901035338224, e-mail: misic@dipteris.unige.it

**Abstract**

The 0-200 m surface layer of the Ross Sea was studied during summer 2014 to demonstrate the lability of the particulate organic matter (POM). With the use of satellite information, we selected three zones, characterised by different physical setting: a northern offshore area, crossing the summer-polynya area of the Ross Sea (hereafter called ROME 1), a more coastal area next to the Terra Nova Bay polynya (ROME 2); a southern offshore area, towards the Ross Ice Shelf (ROME 3). Ice-maps showed that the ice retreat had already occurred. The statistical analysis of the quantitative and qualitative characteristics of the POM pointed to significant differences between the stations, especially in the upper mixed layer (UML). A comparison with previous studies, showed that the localised pulses of the POM accumulation in the UML were similar to those recorded at the highly productive marginal ice zones, providing notable trophic support to the ecosystem. The UML, although rather thin and easily subjected to alterations, confirmed its pivotal role in the ecosystem dynamics. A POM quality favourable to consumers was highlighted at several stations in ROME 1 and ROME 3. Reduced trophic support was, instead, found in ROME 2. A limited POM consumption where deep-water formation takes place, would increase the POM role in the transfer of C to the depths.

**Key Words**

Particulate organic matter, biochemical composition, phytoplankton biomass, physical structure, Ross Sea, Antarctica

## 1. Introduction

Particulate organic matter (POM) is composed of a variety of macromolecules and aggregates, whose dimensions are operationally defined as any material that does not pass through a given filter, usually a 0.45-1 µm (Volkmann and Tanoue, 2002; Verdugo et al., 2004). POM hosts detrital matter as well as living organisms. Ice-algae, phytoplankton, nano- and microzooplankton, and mesozooplankton-derived particles are included in POM. The phytoplankton inside POM forages the trophic web in the open sea, where benthic primary production does not occur, and tight benthic-pelagic coupling therefore plays an important role. On the other hand, the detrital and the heterotrophic microbial components of the POM highlight the fact that this dimensional fraction also has a role in recycling the elements. In addition, POM enters in the transport of C to the deep waters, taking part in the biological pump that regulates C concentrations in the hydrosphere and atmosphere (Luz et al., 2007).

The POM features at any water depth are a function of various interacting processes (e.g. Stemmann et al., 2004), like sinking velocity as determined by particle size and density, fragmentation and consumption by zooplankton and by microorganisms (Kiørboe, 2000, 2001). These processes result in the rapid decrease of bulk POM and the alteration of biochemical POM composition (Suess, 1980; Boyd and Stevens, 2002).

In the Antarctic Ocean, the quantitative features of the POM have been extensively studied (especially chlorophyll-a, particulate organic carbon - POC - and particulate organic nitrogen - PON) (Smith et al., 2000; Smith and Asper, 2001), while detailed information on its lability is rather scarce. The POM may be studied by means of proxies of its nutritional value. The ratios that are commonly used to infer the value of the POM as trophic resource (for instance the POC/PON ratio and the POC/chlorophyll-a ratio) may be implemented by analyses focusing on its caloric content and on the hydrolysable fractions of the POM (Fabiano et al. 1993; Fabiano and Pusceddu, 1998; Misic and Covazzi Harriague, 2008; Kim et al., 2014). The caloric content expresses the actual value of the POM in energy terms. In this case, different biochemical features generate quantitatively different energy values for the POM. For the hydrolysable fraction, biomimetic assays have been developed to evaluate the fraction that may be rapidly hydrolysed by the enzymes commonly found in the environment, to calculate the actual fraction of the POM that is

66 bioavailable to consumers. This approach by-passes the uncertainty of bulk-related analyses (such as POC).
67 In fact, the chemical form of the food supply achieves a high relevance for an efficient biological
68 exploitation. The biomimetic assay allows for the possibility that some compounds may be biochemically
69 refractory to consumption, or physically enclosed in low-lability materials that isolate them from
70 consumers.
71 Interannual, seasonal and spatial variability of biological features is typical of the Antarctic Ocean and the
72 Ross Sea (Smith et al., 1996; Arrigo et al., 1998; Dunbar et al., 1998; Gardner et al., 2000; Saggiomo et al.,
73 2002; Smith et al., 2010; Fragoso and Smith, 2012). However, the mechanisms forcing this spatial
74 heterogeneity are still largely unclear. The presence of ice regulates the onset of primary production, POM
75 accumulation and fluxes in the water column (Garrity et al., 2005). The ice-associated processes physically
76 influence the water column, determining the depth of the upper mixed layer (UML) that is often considered
77 to be a major factor in controlling POM production and distribution (Mangoni et al., 2004; Fragoso and
78 Smith, 2012). Therefore, general trends may be highlighted, based on the degree of maturity of the
79 selected system (Fabiano et al., 2000): closed pack conditions, followed by the Marginal Ice Zone (MIZ)
80 spring conditions, and then by open waters in late spring and summer, generally in the offshore area by late
81 December and in the entire continental shelf region by late January (Comiso et al., 1993, Smith and Asper,
82 2001). Knowing that ice regulates the biological development and, consequently, the features of the POM,
83 other forces must influence the planktonic patterns when ice is lacking, during summer for instance.
84 Although ice may last longer at some sites in the Ross Sea, depending on global climate anomalies as well
85 as local events (Arrigo and van Djiken, 2004), the summer features of the Ross Sea should show less
86 variability than the spring ones. The stratification generated by ice melting should be relaxed due to wind
87 and waves on the open waters, a feature that would allow increased vertical fluxes and a more
88 homogeneous vertical distribution of the POM (Gardner et al., 2000).
89 This study is based on the results of the ROME (Ross Sea Mesoscale Experiment) cruise, carried out during
90 the Antarctic summer of 2014. Sampling was performed focusing on the 0-200 m surface layer of three

areas of the Ross Sea, characterised by different distances from the coast and different mesoscale hydrodynamic structures.

We aimed to: i) highlight whether the quantitative and qualitative features of the POM were homogeneous in the sampled areas, ii) test whether our summer POM features resembled those of previous research performed in the Ross Sea, iii) underline the potential role of the POM in the trophic exchanges and in the global carbon trends of the area.

## 2. Material and methods

### *2.1 Station sites and sampling*

*The in situ* ROME data were collected by the R/V Italica in the framework of the Italian National Program for Antarctic Research (PNRA). Sampling was performed in three different areas of the Ross Sea: ROME 1 was sited at approximately 170°E and 75°S; ROME 2 occupied a more coastward area, next to the Terra Nova Bay (TNB) polynya; ROME 3 was sited in the southern Ross Sea, towards the Ross Ice Shelf, at 168°E (Fig. 1A).

The sampling strategy was defined on the basis of the MODIS (Moderate Resolution Imaging Spectroradiometer) Aqua and Terra satellite level-2 products for the previous 12/24 hours. In particular, the sea surface temperature and surface chlorophyll-a concentration maps at 1 km resolution were analyzed in order to plan and carry out the casts in correspondence with both high and low chlorophyll signals. Additionally, satellite AMSR2 sea ice concentration maps, provided by the University of Bremen, using the ASI sea ice concentration algorithm (Spreen et al., 2008), were considered. In fact, daily maps of the Ross Sea region from early December 2013 to late February 2014 (available at http://www.iup.uni-bremen.de:8084/amsr2) were analyzed to monitor the evolution of the sea ice cover before and during the experiment, in order to study its effects on the physical and biochemical systems.

A total of 46 casts were obtained. Hydrological profiles were acquired by means of a SBE 9/11 Plus CTD, with double temperature and conductivity sensors. For each station the upper mixed layer (UML) depth was determined as the depth at which *in situ* density ($\sigma_t$) changed by 0.05 kg/m$^3$ over a 5 m depth interval.

Current speed and direction were recorded using a Lowered Acoustic Doppler Current Profiler (LADCP) system. Two LADCP were deployed with a CTD, in order to obtain a unique current measurement every 10 m from the surface to the maximum depth reached. The effect of tides on this current dataset was removed following the procedure proposed by Erofeeva et al. (2005).

Water samples for phytoplankton biomass and POM analysis were collected using a Carousel sampler equipped with 24 Niskin bottles (12 L) at 21 stations (Table 1, black circled stations in Fig. 1A).

For the total phytoplankton biomass analysis, the water samples were collected according to the fluorescence signal, to collect samples from the maximum chlorophyll layer. 500 ml of seawater were filtered under low light through Whatman GFF filters (25 mm, nominal pore diameter 0.7 µm), quickly stored at -80 °C until analysis.

For the POM analysis, water samples were collected at 4 fixed depths (surface, 50, 100 and 200 m) and 1 variable depth depending on the maximum of the signal for fluorescence. From 0.5 to 1 L of sampled seawater was filtered through Whatman GFF filters and immediately frozen until analysis in the laboratory.

*2.2 Analytical procedures*

The amount of phytoplankton biomass was estimated from spectrofluorometric analysis on acetone-extracted chlorophyll-a and phaeopigments, following Holm Hansen et al. (1965). The extract was read before and after acidification by using a Varian Eclipse spectrofluorometer, which was checked daily with a chlorophyll-a standard solution (from *Anacystis nidulans* by Sigma). The specific standard deviation of the replicates was based on an average of 4%.

Particulate organic carbon (POC) and particulate organic nitrogen (PON) were analyzed following Hedges and Stern (1984), after acidification with HCl fumes, in order to remove inorganic carbon. Cyclohexanone 2-4-dinitrophenyl hydrazone was used to calibrate a Carlo Erba Mod. 1110 CHN Elemental Analyser. The specific standard deviations due to the analytical procedures and sample handling were 7.4% and 7.8% for POC and PON, respectively.

142 Particulate proteins, carbohydrates and lipids were analyzed following Hartree (1972), Dubois et al. (1956),
143 Bligh and Dyer (1959) and Marsh and Weinstein (1966). Albumin, glucose and tripalmitine solutions were
144 used to calibrate a Jasco V530 spectrophotometer. The specific standard deviations were 8.3%, 15.5% and
145 21.6% for the proteins, carbohydrates and lipids, respectively.
146 Besides the quantitative information given by the single concentration of the different elements and
147 biochemical types, the POC/PON ratio (Huston and Deming, 2002) and the particulate
148 protein/carbohydrate ratio (Misic and Fabiano, 1996) gave clues to the qualitative value of the POM for the
149 consumer. The lowest the POC/PON, and the highest the protein/carbohydrate ratio, the highest the value
150 of the POM as trophic resource.
151 The concentrations of proteins, carbohydrates and lipids were used to calculate the caloric value of the
152 POM (Kcal g $POM^{-1}$) following the Winberg (1971) equation (Kcal g $POM^{-1}$ = 0.055 protein% +0.041
153 carbohydrate% + 0.095 lipid%).
154 The enzyme-hydrolysable fractions of particulate proteins and carbohydrates were determined following
155 the protocols of Gordon (1970), Mayer et al. (1995) and Dell'Anno et al. (2000). The sample filters and filter
156 blanks (Whatman GFF filters not used for filtration) were placed in plastic containers with solutions (100 mg
157 $l^{-1}$ in 0.1 M Na-phosphate buffer) of two selected enzymes purchased from Sigma–Aldrich. Proteinase K was
158 chosen for the hydrolysis of the proteins, β-glucosidase for that of the carbohydrates (Mayer et al., 1995,
159 Dell'Anno et al., 2000). These enzymes are extracted from plants and fungi, but have hydrolytic activities
160 quite similar to natural marine organisms and are widespread among autotrophs and heterotrophs (Dall
161 and Moriarty, 1983). The filters were left in the enzyme solutions for 2 hours, at the optimal temperatures
162 and pH for each enzyme, in order to enhance digestion (Dell'Anno et al., 2000). After hydrolysis, each filter
163 was carefully removed from its container, placed in a filter-holder and rinsed with the solution remaining in
164 the dish and 5ml of deionised water, to return any particles that may have floated off the filter (Gordon et
165 al., 1970). Then the filters were processed for the determinations of proteins and carbohydrates following
166 the same protocols as above. The possibility that the flushing of the buffer could have mechanically
167 removed part of the particulate fraction was avoided by incubating and processing replicates of the

168 samples with only the buffer solution. In addition, an underestimation of the labile proteins and
169 carbohydrates was possible, due to the sorption to minerals or POM (and therefore to their return to the
170 particulate fraction) of the hydrolysed materials. The concentrations detected after hydrolysis, corrected
171 for the eventual error just mentioned (never higher than 20% of the total protein and carbohydrate
172 concentrations), were subtracted from the total concentrations in order to obtain the hydrolysable, or
173 labile, POM. The specific standard deviations were 11.2% and 21.5% for hydrolysable particulate proteins
174 and carbohydrates, respectively.
175
176 *2.3 Data treatment and statistical analysis*
177 The data were divided into a surface layer and a deeper layer, the former defined by the UML depth (Table
178 1) and the latter ranging from the UML depth down to 200 m.
179 The literature data related to previous research carried out in the Ross Sea and TNB were utilised as a
180 comparison. For the Ross Sea Fabiano et al. (2000) provided spring data and Fabiano et al. (1993) and
181 Catalano et al. (1997) early summer data. Fabiano et al. (1995 and 1997) and Povero et al. (2001) provided
182 summer data for the TNB area (Table 2).
183 We tested the differences of the same variable between different samplings with the one-way ANOVA test
184 followed by the Newman-Kneuls *post-hoc* test (ANOVA-NK test) (Statistica software). To test the
185 relationships between the various parameters, a Spearman-rank correlation analysis was performed.
186 The Principal Component Analysis (PCA) was applied to the normalised data of the POC, protein and
187 carbohydrate concentrations and the protein/carbohydrate ratio (PRIMER software). The data were divided
188 into the UML and the deeper layer, as previously described. The ROME data were treated together with the
189 other literature data previously cited (Table 2) to highlight similarities between them. The cluster analysis
190 was performed on the normalised data set (resemblance measure: Euclidean distances, cluster mode:
191 group average), to visually highlight the station grouping. The analysis of similarities (ANOSIM) was applied
192 to highlight significant differences between the groups, while the similarity percentage analysis (SIMPER)
193 was utilised to highlight the parameters responsible for such differences.

194

195 **3. Results**

196 *3.1 Physical properties and sea-ice conditions*

197 The Θ/S diagram obtained from all the sampled stations (Fig. 1B) indicated the presence of several typical
198 Ross Sea shelf water masses. In all the studied areas the surface layer was occupied by the Antarctic
199 Surface Water (AASW), a relatively light surface water characterized by potential temperatures ranging
200 between -1.8°C and +1°C and by salinity values lower than 34.50 (Orsi and Wiederwohl, 2009). In ROME 2
201 (blue circles in Fig. 1B), the AASW core was slightly saltier, colder and denser than expected, with salinity
202 close to 34.60 and potential density lower than 27.9 kg/m$^3$. These values were similar to the Modified
203 Circumpolar Deep Water (MCDW) features, but the high oxygen concentration values (Rivaro et al., 2015)
204 confirmed that we were in the presence of a local AASW.

205 The intermediate and deep layers (from 150 to 1000 m) were occupied by High Salinity Shelf Water (HSSW),
206 and by Terra Nova Bay Ice Shelf Water (TISW), the latter identified only in ROME 2 (Fig. 1B). HSSW is
207 characterized by salinity greater than 34.70, potential temperature near freezing point and potential
208 density greater than 27.9 kg/m$^3$ (Budillon et al., 2003; Rivaro et al., 2014). TISW (from 150 to 350 m) is
209 characterized by potential temperatures below freezing point and salinity values of about 34.70 (Budillon
210 and Spezie, 2000).

211 The physical properties of the upper layer may also be linked to sea ice evolution in the study area. The
212 melting ice in the Ross Sea gradually generates large ice-free areas during summer. Some ROME 1 and
213 ROME 3 stations and all the ROME 2 stations experienced ice-free conditions starting from early December
214 (Figs. 2A and 2B). On the other hand, some stations experienced the presence of ice longer (Figs. 2C and
215 2D). Even in the same sampling area, differences in ice cover can be significant and have an impact on the
216 observed temperature and salinity values. For instance, the northernmost station of ROME 1 (station 20)
217 was covered by ice until 14 January, just 3 days before the sampling. Stations 16 and 18 started to become
218 ice-free from the beginning of January (Fig. 2C). The ROME 3 stations were partially covered by ice until the
219 end of December (Fig. 2B).

220 The vertical structure of the water column of ROME 1 showed deeper UMLs for the stations that
221 experienced longer ice-free conditions (9, 11 and 13, Table 1). In the western stations of ROME 1 the lower
222 depth of the mixed layer depended on the presence of low-salinity surface water, related to the influence
223 of the ice (Fig. 3B). Intensity and direction of the currents along the entire water column (UML shown in
224 Fig. 3D) showed the presence of a northward current along the eastern and western boundary of the leg,
225 while more intense southward velocities were registered in the central part of the leg (stations 13 and 14).
226 The ROME 2 water column was characterized by a UML depth limited to the first 10-15 m (Table 1) due to
227 the presence of a temperature and salinity gradient between the fresher and colder coastal stations and
228 the easternmost, saltier and warmer stations (Figs. 4B and 4C). A frontal structure was visible in the area
229 between stations 45 and 34, where the convergence of the two water masses led to a deepening of the
230 thermocline down to 100 m (Rivaro et al., 2015) and to an abrupt change in the current pattern (Fig. 4D).
231 The strongest current intensities ($p<0.05$) were observed in ROME 3, with values up to 24 cm $sec^{-1}$ for the
232 zonal (u) and meridional (v) components. The current pattern at all depths showed the presence of a
233 cyclonic circulation centred at about 168.5°E 76.45°S (Fig. 5D). This circulation could have increased the
234 UML water mixing, leading to salinity values of 34.23-34.43 and mean temperature values lower than 0.5°C
235 (Figs. 5B and 5C). In fact, the western and central stations (48, 50, 55, 67 and 75) had a more homogeneous
236 water structure for the upper 30-50 m, while stations, placed outside the eddy showed higher surface
237 salinity values and the deepest UML (more than 70 m).
238
239 *3.2 Particulate organic matter*
240 The concentration and distribution of chlorophyll-a in the three areas (Table 3) varied and depended on the
241 physical setting. In ROME 1 the stations characterised by early ice melting showed rather homogeneous
242 chlorophyll-a concentrations in the UML, ranging from 1 to 2 µg $l^{-1}$. Instead, where the halocline was
243 shallower and the stratification stronger (i.e. station 16), a subsurface increase in concentration up to 3 µg
244 $l^{-1}$ was observed, leading to higher average values (Table 3). The chlorophyll-a distribution in ROME 2 was
245 influenced by the previously described hydrological front, associated with the deepening of the

246 thermocline at stations 34 and 45. The frontal structure and the current convergence allowed high
247 chlorophyll-a concentrations at higher depths (values up to 3 µg $l^{-1}$ at 100 m, data not shown). In ROME 3
248 the stations directly influenced by the cyclonic eddy (55, 67 and 75) showed the highest mean chlorophyll-a
249 concentrations (Table 3), with maximum values higher than 4 µg $l^{-1}$.
250 POC values correlated significantly with chlorophyll-a concentrations in ROME 1 and ROME 3 (Table 4).
251 ROME 2, instead, showed no significant correlation, although at 50 and 100 m depths significantly higher
252 POC concentrations ($p<0.05$) than the other two areas were found (Fig 6A).
253 The POC/chlorophyll-a ratio is an indication of the primary biomass contribution to the total POM. The
254 ratios (Table 3) highlighted a generally lower contribution of the photoautotrophic component at the UMLs
255 of ROME 1 and 2, with ratio higher than 150, especially in the stations experiencing longer ice-free
256 conditions (stations 9 and 11 of ROME 1, for instance). In ROME 3 the lowest ratio was, instead, found for
257 the stations lying to the west of the frontal zone.
258 Although the PON and POC concentrations were strongly correlated (Table 4), indicating similar
259 distributions (Figs. 6A and 6B) and likely, the origin of the POC/PON ratio values showed variations with
260 depth (Fig 6C). The POC/PON ratio gives an estimate of the N contribution to the bulk POM, keeping in
261 mind that N-containing molecules are considered attractive to consumers (Huston and Deming, 2002). The
262 highest POC/PON ratio values (above 8) were found in the deeper water layers, especially at stations 9 and
263 11 in ROME 1 and 50, 52, 56, 69 and 75 in ROME 3. The lowest values, below 6, were, instead, found in the
264 UML, especially in ROME 3, where the highest chlorophyll-a values were found. However, significant
265 chlorophyll-a and POC/PON ratio correlations were only found in ROME 2, although this relationship ($r=$
266 0.48, $n=19$, $p<0.05$) highlighted that an increase of autotrophic biomass led to a lowering of the trophic
267 value of the POM.
268 On average, the protein and carbohydrate concentrations showed vertical trends very similar to those of
269 POC (Figs. 6D and 6G). This was also confirmed by the significant correlations found between these
270 variables for the three areas (Table 3). Proteins and carbohydrates also correlated with chlorophyll-a in
271 ROME 1 and 3, while no significant correlation was found in ROME 2. Furthermore, the hydrolysable

fraction of the carbohydrates and lipids was not coupled with the other variables in ROME 2. A reduction of the hydrolysable carbohydrates was, in fact, observed starting from 100 m (Fig. 6H). In this area the lipid concentrations (Fig. 6I) did not show significant decreases with depth (UML vs. deeper layer, $p>0.05$) but rather similar values, significantly lower than in the other areas ($p<0.001$). The contribution of the three POM fractions to POC was reported in Fig. 7A for the UML and the deeper layer. Generally, higher concentrations of residual POC (here called "other POC") were found at the UML, except for stations 34 and 45, that showed a high residual POC fraction also in the deeper layer.

On average, the hydrolysable proteins were 35.4±11.7% of the total proteins (ranging from 6.8 to 75.6%), the hydrolysable carbohydrates 13.1±10.8% of the total carbohydrates (ranging from 0.1 to 44.9%). Generally, the deeper layer contribution of the hydrolysable proteins to POC was higher than the UML one, except for the front-related stations in ROME 2 and station 20 in ROME 1 (Fig 7A). The hydrolysable carbohydrate contribution to POC (Fig.7B) was lower and showed a higher variability in the three areas. In ROME 1, for instance, the contribution showed an inverse trend with chlorophyll-a. The 200-m-deep contributions were higher at the stations not covered by ice from a longer time, than at the stations more recently influenced by ice. ROME 3, however, showed a rather good relationship between the hydrolysable carbohydrate and the phytoplanktonic biomass. The large variability of the hydrolysable carbohydrate contribution to the POC concentration, often visible in Fig. 7B as high standard deviation, implied also strong variations within the UML and the deeper layer that were not found for the hydrolysable proteins.

*3.3 Multivariate statistical analysis*

Fig. 8 shows a PCA plot, where the cluster analysis results are shown as ellipses defined by Euclidean distances. The PC1 axis explained 71% of the variation, while the PC2 explained a further 24%. Two significantly different main groups (ANOSIM analysis, Table 5) were observed: the main part of the UML observations belonged to the richer group A, while the deeper layer observations were clustered in group B. Proteins and carbohydrates explained the major part of this difference (SIMPER analysis, Table 5). The

297 group B stations showed POC concentrations 3.4-fold lower than the observations of group A, 4.8 for
298 proteins and 2.8 for carbohydrates.
299 In group A the samples were organised into two main sub-groups: a1 and a2. The multivariate analyses
300 highlighted significant differences between them (ANOSIM analysis, Table 5), mainly due to the different
301 ratios between proteins and carbohydrates (explaining 41% of the difference, SIMPER analysis, Table 5). In
302 group B two more sub-groups were recorded, differing significantly (ANOSIM analysis, Table 5) due to the
303 carbohydrate concentrations (explaining 47% of the difference, SIMPER analysis, Table 5).
304 Each sub-group had a particular signature, defined by the previous studies carried out in the area (Table 2):
305 sub-group a1 clustered the MIZ stations (8, 10, 28, 30) and the spring polynya station MP, sub-group a2 the
306 coastal TNB stations. The surface observations characterised by a closed-pack coverage (27 and 29)
307 belonged to sub-group b1, together with the main part of the deeper layer observations; sub-group b2
308 collected those of the early summer polynya stations (15, 17, 19, 21) and the deeper coastal layer
309 observations (TNB).
310
311 *3.4 Caloric value analysis*
312 The caloric value of the POM in the two water layers was only calculated for stations where the lipid
313 analysis was carried out, namely 9, 13, 16 and 20 of ROME 1, 34, 39 and 45 of ROME 2 and 50, 55 and 67 of
314 ROME 3. The plot of these results, with the previous research carried out in the Ross Sea and at the coastal
315 TNB (Table 2) is presented in Fig. 9. In this figure we have merged the bulk quantitative (POC) and
316 qualitative (caloric value) information on the POM.
317 During previous research, it was noticed a rising trend of the quantitative features in the UML from the
318 poorer pack-ice zones to the polynya and then to the MIZ, ending with the richer coastal sites, although the
319 MIZ could also show high concentrations of POM of moderate caloric values. The previous pack-ice
320 observations showed that low concentrations were associated with an average caloric value, while the
321 qualitative value of the other stations was higher (MIZ and coastal) or lower (polynya).

322 The stations in ROME 2 matched the quantitative and qualitative features of the polynya in the entire water
323 column. The surface observations of the other areas were grouped with the MIZ and previous coastal
324 observations for the UML. The deeper layer observations in the ROME 1 and ROME 3 areas resembled
325 those of the MIZ, spring polynya and deeper pack-layer, although their caloric value was higher.
326
327 **4. Discussion**
328 *4.1 Quantitative and qualitative features of the summer POM: a comparison with previous studies in the*
329 *Ross Sea*
330 The study of the features and role of the POM in the ecosystem may be approached at different levels. The
331 first level we tested was focused on the quantitative characteristics of POM at different stations (PCA -
332 multivariate analysis, Fig. 8). Although the UML was rather thin at several stations, significant quantitative
333 differences were observed between the two water layers (Table 5), with a sharp reduction in POM in the
334 deeper layer, already established by the observations by Nelson et al. (1996), Fabiano et al. (2000) and
335 Gardner et al. (2000) for the Ross Sea. They stated that the primary production is recycled in the photic
336 layer and only a small part will sink to the bottom, following the concept of a "retentive system". The
337 grouping of the observations of the two layers, as revealed by multivariate analysis, indicated a strong and
338 significant variability in the UML, while the deeper layer was more homogeneous, also when compared to
339 observations from other years and seasons, except for ROME 2.
340 Except for the northern stations of ROME 1 (18 and 20), ice-free water conditions were established in the
341 whole ROME sampling area from the beginning of January, at least two weeks before the sampling.
342 Therefore, open water conditions, resembling those of the previous spring-summer polynya/open water
343 observations, were common in the entire area. On the contrary, the multivariate analysis performed on
344 POM indicated polynya/open-water features for the UML as well as similarity to the previous MIZ ones,
345 pointing to heterogeneity.
346 The sub-group a1 linked some stations of the ROME cruise and the previously studied spring polynya
347 station MP. Nevertheless, Fabiano et al. (2000) observed that this station was part of a more complex

348 period of melting-ice. This may explain why this station was also grouped with the spring MIZ ones in the
349 PCA plot. The MIZ stations were generally characterised by high POM productivity (Saggiomo et al., 1998;
350 Fitch and Moore, 2007), being the priming for further planktonic development. The multivariate statistical
351 analysis indicated that these stations showed rather high POM concentrations and, in particular, the
352 highest prevalence of proteins over carbohydrates. It is well known that N-rich proteins cover multiple roles
353 (energetic, functional, structural) and thus a high protein concentration indicates a good food supply for
354 consumers (Etcheber et al., 1999). Particulate carbohydrates, instead, generally have a lower lability,
355 because they also encompass complex structural polysaccharides whose digestion is energy-expensive,
356 slowing their consumption rates (Pusceddu et al., 2000). One of the main processes that enrich the POM of
357 proteins is microbial activity. Microbial heterotrophic reworking of autotrophic and detrital POM, generally
358 performed by bacteria, increases the N content of the detritus (Povero et al., 2003) and of the autotrophic
359 colonies (Carlson et al., 1998) especially during summer. A general and marked dominance of proteolysis
360 over other classes of hydrolytic enzymes has been previously reported (Misic et al., 2002; Celussi et al.,
361 2009), indicating an efficient N-recycling by unicellular heterotrophs. The conversion of detrital-N into high
362 trophic value biomass is completed by an efficient microbial-loop, recovering a large part of the DOM
363 released during phytoplanktonic blooming (Kirchman et al., 2001). In addition, Sala et al. (2005) found that
364 bacteria might utilise other DOM sources (in particular dissolved carbohydrates), thus increasing their
365 efficiency in biomass accumulation. The rather low POC/PON ratio values we found compared, for instance,
366 to Smith et al. (2000) (on average for the upper 100 m layer they found summer values of 6.9±0.5 vs. our
367 5.8±0.3 and 6.4±0.9 calculated for the UML and 0-200 m layer, respectively), are consistent with micro-
368 heterotrophic presence, as bacterial standing stock can be considered as the amount of particulate organic
369 matter possessing high nutritional quality (Monticelli et al., 2003).
370 Another process that may increase the protein concentration is the phytoplankton bloom with a high
371 constitutive protein content. For instance, in cold waters the diatom protein content is approximately
372 double that of temperate waters (Young et al., 2015). The very high chlorophyll-a concentrations of some

373 of these stations (48, 56 and 75 for instance) agree with this second hypothesis, bringing these stations
374 closer to the highly productive spring season.
375 The other UML observations of the ROME cruise (sub-group a2) resembled the coastal features of TNB
376 during summer, showing the highest concentrations of POM, although their quality as food supply for
377 consumers was lower than that of sub-group a1.
378 In our study, a clear relationship between physical forcing, phytoplankton biomass and POM accumulation
379 was provided by ROME 3. In this case, the UML depth (generally deeper than 30 m in our study) exerted a
380 lower influence on the POM production and accumulation than that observed by Fragoso and Smith (2012),
381 who noted that the shallower mixed layer depths (<20 m) in late spring and early summer appeared to
382 promote diatom growth. The phytoplankton biomass was pivotal for the POM composition. In fact, it
383 regulated the POM quantitative features, as revealed by the highly significant correlations between the
384 chlorophyll-a and the quantitative variables of the POM (Table 4) (Davis and Benner, 2005) and by the
385 POC/chlorophyll-a ratio values for the stations on the western side of the area (eddy-influenced zone), that
386 were significantly lower ($p<0.05$) than the other ROME areas. Young et al. (2015) found that Antarctic
387 diatoms take up to 50% of biomass to protein, explaining the very high significance of the correlation.
388 Arrigo and van Djiken (2004) described the area of ROME 3 as a boundary between spring and summer
389 blooms, a kind of frontal area that may show an unusually high chlorophyll-a accumulation at the surface,
390 depending on general atmospheric conditions over the entire Ross Sea. The blooming we observed was
391 influenced by the peculiar physical constraints of this area, such as the presence of a frontal area and a
392 cyclonic eddy that divided some of the richer north-western stations from the others. The water mixing of
393 the UML, due to the more intense hydrodynamic forcing, fertilised the surface layer, probably stripped of
394 nutrients by earlier spring blooms. In addition, a higher instability in the water column, that is known to
395 influence phytoplankton development, could have favoured some species that, before, were limited by
396 competition (Fonda Umani et al., 2002).
397 Our observations point to the pivotal role of the summer autotrophic processes, providing a large
398 accumulation of biomass and strongly sustaining the ecosystem. This feature was unclear in the multi-year

399 comparison by Arrigo and van Djiken (2004) and in the studies by Smith and Asper (2001) and Rigual-
400 Hernandez et al. (2015), who observed a general decrease in chlorophyll-a concentrations from spring to
401 summer in normal years. In addition, the POC/chlorophyll-a ratios of our study were significantly lower
402 ($p<0.05$) than those reported by Smith et al. (2000) for the Ross Sea in summer, while they were similar to
403 the values the same authors reported for spring. This confirmed the pivotal role of the living phytoplankton
404 fraction during summer in the UML of the Ross Sea, where mesoscale hydrological structures occur.
405 The last sub-group showing polynya features is the b2 of the PCA. In this group station 20 of ROME 1 the
406 features of the early summer polynya stations were matched, despite the fact that it was ice-free for a
407 shorter time than the others. Horizontal advection of POM from the adjacent areas could have provided
408 the concentrations we found (Rigual-Hernández et al., 2015). The heavier ice-influence could have favoured
409 the accumulation and persistence of sympagic-derived materials, as indicated by the rather high surface
410 chlorophyll-a concentrations.
411
412 *4.2 Caloric value of summer POM*
413 The plotting of the POC with the POM caloric value (Fig. 9) provides information on the energy potentially
414 provided to heterotrophic consumers by the POM.
415 The ROME stations that resemble the spring and early-summer features of the polynya were those of
416 ROME 2. Actually, these stations experienced real polynya environmental conditions, being next to the TNB
417 polynya. The ROME 2 stations had low caloric values in the entire water column, although, from a
418 quantitative point of view, some of them in the UML had similar features to the richer coastal areas (sub-
419 group a2 of Fig 8). In the entire water column, POM maintained the same caloric content of the mixed
420 layer, as previously found for the coastal TNB (Fabiano et al., 1996), when the caloric value was on average
421 5.33 Kcal/g. This is not really very high, due to the high contribution of carbohydrates that have the lowest
422 caloric value among the three biochemical components. We observed that in ROME 2 the chlorophyll-a was
423 associated with carbonaceous POM (it correlated positively to the POC/PON ratio), therefore in this area

424 the freshly-produced summer POM had different features, namely a lower trophic value, than the offshore
425 area.
426
427 *4.3 Hydrolysable proteins and carbohydrates of summer POM*
428 Generally, the hydrolysable protein contribution was rather low during the ROME cruise, on average 35% of
429 the total proteins. This was clearly lower than the contribution (higher than 90%) observed at coastal
430 stations in the NW Mediterranean (Misic and Covazzi Harriague, 2008), and by Fabiano and Pusceddu
431 (1998), who observed that 50% of the total proteins in TNB were hydrolysable. Besides the possibility that
432 actual variations in time and space may occur, these differences may be due to the fact that the cited
433 authors used trypsin to hydrolyse proteins, while in the present study, we used proteinase K. The
434 hydrolysable carbohydrate contribution to total carbohydrates, instead, showed average values similar to
435 those recorded in the previously cited NW Mediterranean (from 5 to 30%), but notably lower than the 80%
436 found in TNB using the same method and hydrolytic enzyme. This pointed to sharp spatial variations of the
437 hydrolysable fraction of POM from the actual coastal area (Fabiano and Pusceddu, 1998) to the offshore
438 area next to the polynya of TNB (this study). The vertical trends of the hydrolysable carbohydrates in the
439 three ROME areas were different, reflecting a general influence by the environmental features on the
440 distribution of the hydrolysable carbohydrate, but the relatively small size of our data set prevented deeper
441 analysis of this item.
442 The main contribution to POC was given by the hydrolysable proteins, that showed slight, but interesting
443 differences between the ROME areas and in the same area, following the mesoscale physical features.
444 Assuming that the POM production in the Ross Sea has a main phytoplankton signature (Fragoso and Smith,
445 2012), the fresh (generally more labile) POM should be found at the surface at the beginning of the
446 productive season (spring), but the POM vertical fluxes of summer and the proliferation of the bacterial
447 biomass would increase the quantity of labile heterotrophic materials such as proteins in the depth.
448 At the ROME sites the contribution of the labile proteinaceous C to the POC was, generally, higher in the
449 deeper layer than in the mixed layer (Fig. 7A). In ROME 1 this proved true for the stations that had

450 experienced longer ice-free conditions. Generally, in such areas, the relaxing of the stratification due to
451 wind and waves allows a more homogeneous vertical distribution of POM by water-mass physical mixing.
452 The lower maturity of station 20 (namely a higher ice-influence as revealed by salinity), instead, led to
453 conditions more similar to spring, with a higher labile contribution at the surface.
454 ROME 2, instead, showed peculiar features. Despite being ice-free for the longest time and lying next to the
455 winter polynya of TNB, its stations displayed a lower labile contribution in the deeper layer than in the
456 UML. Station 39 was an exception, lying to the east of the hydrological front and being influenced by an
457 offshore current coming from the ROME 1 area. The other stations were separated from the actual offshore
458 area by the front found at stations 34 and 45.
459 The vertical transport of the POM by vertical water mixing has a double relevance: it is essential for the
460 foraging of bottom and mesopelagic communities, and it may contribute to the $CO_2$ biological pump. The
461 occurrence of vertical transport, as shown by the ROME 2 and coastal observations in terms of bulk POM,
462 may improve deep-sea trophism, but also push C into the deep current system via the bottom-water. The
463 vertical distribution of POM at the ROME 2 stations pointed to an efficient biological pump, because the
464 POM accumulation was observed down to 200 m. The TNB area is characterised by the formation of dense
465 water masses due to brine release during sea-ice production (HSSW) and by the freshening and cooling of
466 the HSSW due to contact with the ice shelf (TISW). HSSW fills-up the deeper layer of the Drygalsky Basin
467 and flows northwards until it reaches the shelf-break, which overflows down the continental slope,
468 ventilating to the abyssal depths near Cape Adare (Jacobs et al., 1970; Withworth and Orsi, 2006; Budillon
469 et al., 2011). The deep layer POM of ROME 2 was more refractory, showing proportionally lower
470 hydrolysable proteins and carbohydrates, higher POC/PON ratio, lower protein/carbohydrate ratio and a
471 lower caloric content than the mixed layer. If refractivity is a limiting factor for the biological respiration of
472 POM, it allows a more efficient burial of not respired C to the depth, indicating TNB as a sink for C in
473 summer (Fonda Umani et al., 2002).
474
475 **5. Conclusions**

476 In this study, we firstly aimed at determining whether the POM was uniformly distributed in the Ross Sea
477 area during a particular season (summer), when one of the main constraints regulating POM production
478 and consumption (namely the ice cover) was generally lacking. We found that heterogeneity was still a
479 dominant feature of the Ross Sea, due to the mesoscale characteristics of each area. The presence of fronts
480 and eddies, with high current intensities, mixed the UML, stimulating phytoplankton production and POM
481 accumulation. Nevertheless, the vertical and horizontal extent of this fertilisation was not continuous. The
482 offshore ROME 1 and 3 areas differed from the ROME 2 area, especially with regards to the qualitative
483 features of the POM. The deeper-layer POM was found to have higher lability in ROME 1 and 3, while the
484 more coastal ROME 2 had inverse features. This may be relevant, because the POM of the deeper water,
485 which would likely join the dense-water journey to the abyssal depths of the oceans, has a potentially lower
486 trophic value and could be respired to a lesser extent, contributing to C storage in the bottom. On the other
487 hand, enrichment of the deeper POM of the other areas via bacterial growth and high protein-containing
488 phytoplankton would increase its trophic value, providing a valuable source of materials and energy for
489 those consumers that also maintain a certain metabolic activity during winter.
490 This study also highlighted that the heterogeneity of the offshore areas was principally a matter of the
491 UML. This is a critical point, because the surface layer is the first to be influenced by climatic changes. Small
492 atmospheric changes could lead to increased ecological changes, altering the fragile balance of the
493 Southern Ocean.
494

495 **Acknowledgements**
496 We would like to thank the captain and crew of the R/V Italica for their unstinting assistance during the
497 cruise. We are grateful to Paolo Povero and Enrico Olivari for their logistical support and for the hard
498 sampling work, to Paola Rivaro, who provided the UML depths, and to Giorgio Budillon for the constructive
499 discussion on the physical data. This study was conducted in the framework of the project “Ross Sea
500 Mesoscale Experiment (ROME)” funded by the Italian National Program for Antarctic Research (PNRA,
501 2013/AN2.04).

502

503 **References**


504 Arrigo, K.R., Worthen, D., Schnell, A., Lizotte, M.P., 1998. Primary production in Southern Ocean Waters. J.
505 Geophys. Res. 103, 15587–15600.

506 Arrigo, K.R., van Djiken, G.L., 2004. Annual changes in sea-ice, chlorophyll a, and primary production in the
507 Ross Sea, Antarctica. Deep-Sea Res. I 51, 117–138.

508 Bligh, E.G., Dyer, W.J., 1959. A rapid method of total lipid extraction and purification. Can. J. Biochem.
509 Physiol. 37, 911–917.

510 Boyd, P.W., Stevens, C.L., 2002. Modelling particle transformations and the downward organic carbon flux
511 in the NE Atlantic Ocean. Progr. Oceanogr. 52, 1–29.

512 Budillon, G., Spezie, G., 2000. Thermohaline structure and variability in the Terra Nova Bay polynya, Ross
513 Sea. Antarct. Sci. 12, 493–508.

514 Budillon, G., Castagno, P., Aliani, S., Spezie, G., Padman, L., 2011. Thermohaline variability and Antarctic
515 bottom water formation at the Ross Sea shelf break. Deep-Sea Res. Part I, 1002–1018.

516 Budillon, G., Pacciaroni, M., Cozzi, S., Rivaro, P., Catalano, G., Ianni, C., Cantoni, C., 2003. An optimum
517 multiparameter mixing analysis of the shelf waters in the Ross Sea. Antarct. Sci. 15,105-118.

518 Carlson, C.A., Ducklow, H.W., Hansell, D.A., Smith, W.O., 1998. Organic carbon partitioning during spring
519 phytoplankton blooms in the Ross Sea polynya and the Sargasso Sea. Limnol Oceanogr. 43 (3), 275-
520 386.

521 Catalano, G., Povero, P., Fabiano, M., Benedetti, F., Goffart, A., 1997. Nutrient utilisation and particulate
522 organic matter changes during summer in the upper mixed layer (Ross Sea, Antarctica). Deep-Sea
523 Res. I 44, 97–112

524 Celussi, M., Cataletto, B., Fonda Umani, S., Del Negro, P., 2009. Depth profiles of bacterioplankton
525 assemblages and their activities in the Ross Sea. Deep-Sea Res. I 56, 2193–2205.

526 Comiso, J.C., McClain, C.R., Sullivan, C.W., Ryan, J.P., Leonard, C.L., 1993. Coastal Zone Color Scanner
527 pigment concentrations in the Southern Ocean and relationships to geophysical surface features. J.
528 Geophys. Res. 98, 2419-2451.
529 Dall, W., Moriarty, D.J.W., 1983. Functional aspects of nutrition and digestion. In: Mantel, L.H. (Ed.), The
530 Biology of Crustacea, vol. 5. Academic Press, New York, pp. 215–261.
531 Davis, J., Benner, R., 2005. Seasonal trends in the abundance, composition and bioavailability of particulate
532 and dissolved organic matter in the Chukchi/Beaufort Seas and western Canada Basin. Deep-Sea Res.
533 II 52, 3396–3410.
534 Dell'Anno, A., Fabiano, M., Mei, M.L., Danovaro, R., 2000. Enzymatically hydrolysed protein and
535 carbohydrate pools in deep-sea sediments: estimates of the potentially bioavailable fraction and
536 methodological considerations. Mar. Ecol. Progr. Ser. 196, 15–23.
537 Dubois, M., Gilles, K.A., Hamilton, J.K., Rebers, P.A., Smith, F., 1956. Colorimetric method for determination
538 of sugars and related substances. Anal. Chem. 39, 350-356.
539 Dunbar, R.B., Leventer, A.R., Mucciarone, D.A., 1998. Water column sediment fluxes in the Ross Sea,
540 Antarctica: atmospheric and sea ice forcing. J. Geophys. Res. 103 (30), 741-759.
541 Erofeeva, S.Y., Egbert, G.D., Padman, L., 2005: Assimilation of ship-mounted ADCP data for barotropic tides:
542 Application to the Ross Sea, J. Atmos. Oceanic Technol., 22: 721-734.
543 Etcheber, H., Relexans, J.-C., Beliard, M., Weber, O., Buscail, R., Heussner, S., 1999. Distribution and quality
544 of sedimentary organic matter on the Aquitanian margin (Bay of Biscay). Deep-Sea Res. 46, 2249-
545 2288.
546 Fabiano, M., Pusceddu A., 1998. Total and hydrolizable particulate organic matter (carbohydrates, proteins
547 and lipids) at a coastal station in Terra Nova Bay (Ross Sea, Antarctica). Polar Biol. 19,125-132.
548 Fabiano, M., Povero, P., Danovaro, R., 1993. Distribution and composition of particulate organic matter in
549 the Ross Sea (Antarctica). Polar Biol.13, 525–533.

550 Fabiano, M., Danovaro, R., Crisafi, E., La Ferla, R., Povero, P., Acosta-Pomar, L., 1995. Particulate matter
551 composition and bacterial distribution in Terra Nova Bay (Antarctica) during summer 1989-1990.
552 Polar Biol. 15, 393-400.
553 Fabiano, M., Povero, P., Danovaro, R., 1996. Particulate organic matter composition in Terra Nova Bay (Ross
554 Sea, Antarctica) during summer 1990. Antarct. Sci. 8, 7–13.
555 Fabiano, M., Chiantore, M., Povero, P., Cattaneo-Vietti, R., Pusceddu, A., Misic, C., Albertelli, G., 1997.
556 Short-term variation in particulate matter flux in Terra Nova Bay, Ross Sea. Antarct. Sci. 9, 143-149.
557 Fabiano, M., Povero, P., Misic, C. 2000. Spatial and temporal distribution of particulate organic matter in
558 the Ross Sea. In Faranda, F.M., Guglielmo, L., Ianora, A. (Eds.) Ross Sea ecology. Berlin: Springer, pp.
559 135–150.
560 Fitch, D. T., Moore, J. K., 2007. Wind speed influence on phytoplankton bloom dynamics in the Southern
561 Ocean Marginal Ice Zone, J. Geophys. Res. 112, C08006, doi:10.1029/2006JC004061.
562 Fonda Umani, S., Accornero, A., Budillon, G., Capello, M., Tucci, S., Cabrini, M., Del Negro, P., Monti, M., De
563 Vittor, C., 2002. Particulate matter and plankton dynamics in the Ross Sea Polynya of Terra Nova Bay
564 during the austral summer 1997/1998. J. Mar. Syst. 36, 29–49.
565 Fragoso, G.M., Smith Jr., W.O., 2012. Influence of hydrography on phytoplankton distribution in the
566 Amundsen and Ross Seas, Antarctica. J. Mar. Syst. 89, 19–29.
567 Gardner, W.D., Richardson, M.J., Smith Jr., W.O., 2000. Seasonal patterns of water column particulate
568 organic carbon and fluxes in the Ross Sea, Antarctica. Deep-Sea Res. 47, 3423-3449.
569 Garrity, C., Ramseier, R.O., Peinert, R., Kern, S., Fischer, G., 2005. Water column particulate organic carbon
570 modeled fluxes in the ice-frequented Southern Ocean. J. Mar. Syst. 56, 133– 149.
571 Gordon Jr., D.C., 1970. Some studies on the distribution and composition of particulate organic carbon in
572 the North Atlantic Ocean. Deep-Sea Res. 17, 233–243.
573 Hartree, E.F., 1972. Determination of proteins: a modification of the Lowry method that gives a linear
574 photometric response. Anal. Biochem. 48, 422–427.

575 Hedges, J.I., Stern, J.H., 1984. Carbon and nitrogen determination of carbonate-containing solids. Limnol.
576 Oceanogr. 29, 657–663.
577 Holm-Hansen, O., Lorenzen, C.J., Holmes, R.W., Strickland, J.D.H., 1965. Fluorometric determination of
578 chlorophyll. J. Cons. Perm. Int. Explor. Mer. 30, 3-15.
579 Huston, A.L., Deming, J.W., 2002. Relationships between microbial extracellular enzymatic activity and
580 suspended and sinking particulate organic matter: seasonal transformations in the North Water.
581 Deep-Sea Res. II 49, 5211–5225.
582 Jacobs, S.S., Amos, A.F., Bruchhausen, P.M., 1970. Ross Sea oceanography and Antarctic Bottom Water
583 formation. Deep-Sea Res. 17, 935–962.
584 Kim, B.K., Lee, J.H., Yun, M.S., Joo, H.T., Song, H.J., Yang, E.J., Chung, K.H., Kang, S.-H., Lee, S.H., 2014. High
585 lipid composition of particulate organic matter in the northern Chukchi Sea, 2011. Deep- Sea Res. II,
586 120, 72-81. DOI: 10.1016/j.dsr2.2014.03.022i
587 Kiørboe, T., 2000. Colonization of marine snow aggregates by invertebrate zooplankton: abundance,
588 scaling, and possible role. Limnol. Oceanogr. 45, 479–484.
589 Kiørboe, T., 2001. Formation and fate of marine snow: small scale processes with large-scale implications.
590 Sci. Mar. 65, 57–71.
591 Kirchman, D.L., Meon, B., Ducklow, H.W., Carlson, C.A., Hansell, D.A., Steward, G.F., 2001. Glucose fluxes
592 and concentrations of dissolved combined neutral sugars (polysaccharides) in the Ross Sea and Polar
593 Front Zone, Antarctica. Deep-Sea Res. II 48, 4179–4197.
594 Lutz, M.J., Caldeira, K., Dunbar, R.B., Behrenfeld, M.J., 2007. Seasonal rhythms of net primary production
595 and particulate organic carbon flux to depth describe the efficiency of biological pump in the global
596 ocean. J. Geophys. Res. 112, C10011.
597 Mangoni, O., Modigh, M., Conversano, F., Carrada, G.C., Saggiomo, V. 2004. Effects of summer ice coverage
598 on phytoplankton assemblages in the Ross Sea, Antarctica. Deep-Sea Res. I 51 (11): 1601-1617.
599 Marsh, J.B., Weinstein, D.B., 1966. A simple charring method for determination of lipids. J. Lipid Res. 7, 574-
600 576.

601 Mayer, L.M., Schick, L.L., Sawyer, T., Plante, C.J., Jumars, P.A., Self, R.L., 1995. Bioavailable amino acids in
602 sediments: a biomimetic, kinetics, based approach. Limnol. Oceanogr. 40, 511–520.
603 Misic, C., Covazzi Harriague, A., 2008. Organic matter recycling in a shallow coastal zone (NW
604 Mediterranean): the influence of local and global climatic forcing and organic matter lability on
605 hydrolytic enzyme activity. Cont. Shelf Res. 28, 2725-2735.
606 Misic, C., Fabiano, M., 1996. A functional approach to the assessment of the nutritional value of the
607 particulate organic matter. Chem. Ecol. 13, 51–63.
608 Misic, C., Povero, P., Fabiano, M., 2002. Ectoenzymatic ratios in relation to particulate organic matter
609 distribution (Ross Sea, Antarctica). Microb. Ecol. 44, 224–234.
610 Monticelli, L.S., La Ferla, R., Maimone, G., 2003. Dynamics of bacterioplankton activities after a summer
611 phytoplankton bloom period in Terra Nova Bay. Antarctic Sci. 15, 85–93.
612 Nelson, D.M., Demaster, D.J., Dunbar, R.B., Smith Jr., W.O., 1996. Cycling of organic carbon and biogenic
613 silica in the Southern Ocean: estimates of water-column and sedimentary fluxes on the Ross Sea
614 continental shelf. J. Geophys. Res. 10, 18519–18532.
615 Orsi, A.H., Wiederwohl, C.L., 2009. A recount of Ross Sea waters. Deep-Sea Res. II 56, 778-795.
616 doi:10.1016/ j.dsr2.2008.10.033
617 Povero, P., Chiantore, M., Misic, C., Budillon, G., Cattaneo-Vietti, R., 2001. Land forcing controls pelagic-
618 benthic coupling in Adélie Cove (Terra Nova Bay, Ross Sea). Polar Biol. 24, 875–882.
619 Povero, P., Misic, C., Ossola, C., Castellano, M., Fabiano, M., 2003. The trophic role and ecological
620 implications of oval faecal pellets in Terra Nova Bay (Ross Sea). Polar Biol. 26, 302–310.
621 Pusceddu, A., Dell'Anno, A., Fabiano, M. 2000. Organic matter composition in coastal sediments at Terra
622 Nova Bay (Ross Sea) during summer 1995. Polar Biol. 23:288–293.
623 Rigual-Hernández, A.S., Trull, T.W., Bray, S.G., Closset, I., Armand, L.K., 2015. Seasonal dynamics in diatom
624 and particulate export fluxes to the deep sea in the Australian sector of the southern Antarctic Zone.
625 J. Mar. Syst. 142, 62–74.

626 Rivaro, P., Messa, R., Ianni, C., Magi, E., Budillon, G., 2014. Distribution of total alkalinity and pH in the Ross
627 Sea (Antarctica) waters during austral summer 2008. Polar Res. 33, 20403.
628 http://dx.doi.org/10.3402/polar.v33.20403.
629 Rivaro, P., Ianni, C., Langone, L., Ori, C., Aulicino, G., Cotroneo, Y., Saggiomo, M., Mangoni, O., 2015.
630 Physical and biological forcing on the mesoscale variability of the carbonate system in the Ross Sea
631 (Antarctica) during the summer season 2014. J. Mar. Syst., doi: 10.1016/j.jmarsys.2015.11.002.
632 Saggiomo, V., Carrada, G.C., Mangoni, O., Ribera d'Alcalà, M., Russo, A., 1998. Spatial and temporal
633 variability of size-fractionated biomass and primary production in the Ross Sea (Antarctica) during
634 austral spring and summer. J Mar. Syst. 17, 115–127.
635 Saggiomo, V., Catalano, G., Mangoni, O., Budillon, G., Carrada, G.C., 2002. Primary production processes in
636 ice-free waters of the Ross Sea (Antarctica) during the austral summer 1996. Deep-Sea Res. II 49,
637 1787–1801.
638 Sala, M.M., Arin, L., Balagué, V., Felipe, J., Guadayol, Ò., Vaqué, D., 2005. Functional diversity of
639 bacterioplankton assemblages in western Antarctic seawaters during late spring. Mar. Ecol. Prog. Ser.
640 292, 13–21.
641 Smith Jr, W.O., Nelson, D.M., Di Tullio, G.R., Leventer, A.R., 1996.Temporal and spatial patterns in the Ross
642 Sea: phytoplankton biomass elemental composition, productivity and growth rates. J. Geophys. Res.
643 101, 18455–18466.
644 Smith Jr., W.O., Asper, V.A., 2001. The influence of phytoplankton assemblage composition on
645 biogeochemical characteristic and cycles in the Southern Ross Sea, Antarctica. Deep-Sea Res. I 48,
646 137–161.
647 Smith Jr., W.O., Marra, J., Hiscock, M.R., Barber, R.T., 2000. The seasonal cycle of phytoplankton biomass
648 and primary productivity in the Ross Sea, Antarctica. Deep-Sea Res. II 47, 3119–3140.
649 Smith Jr., W.O., Dinniman, M.S., Tozzi, S., DiTullio, G.R., Mangoni, O., Modigh, M., Saggiomo, V., 2010.
650 Phytoplankton photosynthetic pigments in the Ross Sea: patterns and relationships among functional
651 groups .J. Mar. Syst. 82, 177–185.

652 Spreen, G., Kaleschke, L., Heygster, G., 2008. Sea ice remote sensing using AMSR-E 89 GHz channels *J.*
653 Geophys. Res., vol. 113, C02S03, doi:10.1029/2005JC003384.
654 Stemmann, L., Jackson, G.A., Ianson, D., 2004. A vertical model of particle size distributions and fluxes in
655 the midwater column that includes biological and physical processes–Part I: model formulation.
656 Deep-Sea Res. I 51, 865–884.
657 Suess, E., 1980. Particulate organic carbon flux in the oceans—surface productivity and oxygen utilisation.
658 Nature 288, 260–263.
659 Verdugo, P., Alldredge, A.L., Azam, F., Kirchman, D.L., Passow, U., Santschi, P.H., 2004. The oceanic gel
660 phase: a bridge in the DOM–POM continuum. Mar. Chem. 92, 67-85.
661 Volkman, J.K., Tanoue, E. 2002. Chemical and biological studies of particulate organic matter in the ocean. J.
662 Oceanogr. 58, 265-279.
663 Winberg, G.G., 1971. Symbols, units and conversion factors in study of fresh waters productivity. Int. Biol.
664 Programme, 23.
665 Whitworth T., Orsi, A.H., 2006. Antarctic Bottom Water production and export by tides in the Ross Sea,
666 Geophys. Res. Lett. 33, L12609,doi:10.1029/2006GL026357
667 Young, J.N., Goldman, J.A.L., Kranz, S.A., Tortell, P.D., Morel, F.M.M., 2015. Slow carboxylation of Rubisco
668 constrains the rate of carbon fixation during Antarctic phytoplankton blooms. New Phytol. 205, 172–
669 181. doi: 10.1111/nph.13021
670

671 **Captions to figures**

672

673 Fig. 1. A: Map of the stations of the ROME 1 (red dots), ROME 2 (blue dots) and ROME 3 (green dots) areas.
674 Black-circled points indicate the POM sampling stations. B: Θ/S diagram obtained from the entire available
675 dataset indicates the main water masses. Data from the three different areas (ROME 1, ROME 2 and ROME
676 3) are represented with different colours (red, blue and green, respectively).

677

678 Fig. 2. Sea-ice concentration maps of the Ross Sea for 1 December (A), 19 December (B), 7 January (C), 14
679 January (D). Red circles and numbers highlight the position of the ROME 1, ROME 2 and ROME 3 sampling
680 areas.

681

682 Fig. 3. Station map (A) and maps of mean salinity (B), temperature (C) and currents (D) in the upper mixed
683 layer at ROME 1.

684

685 Fig. 4. Station map (A) and maps of mean salinity (B), temperature (C) and currents (D) in the upper mixed
686 layer at ROME 2.

687

688 Fig. 5. Station map (A) and maps of mean salinity (B), temperature (C) and currents (D) in the upper mixed
689 layer at ROME 3.

690

691 Fig. 6. Vertical profiles of the variables averaged for each depth at each area (standard deviations are
692 reported). A: particulate organic carbon (POC), B: particulate organic nitrogen (PON), C: particulate organic
693 carbon/particulate organic nitrogen ratio (POC/PON), D: particulate proteins (PRT), E: hydrolysable
694 particulate proteins (h-PRT), F: particulate proteins/carbohydrate ratio (PRT/CHO), G: particulate
695 carbohydrates (CHO), H: hydrolysable particulate carbohydrates (h-CHO), I: particulate lipids (LIP).

696

Fig. 7. (A) Contribution of proteins (white), carbohydrates (light grey) and lipids (grey) to POC in the UML (U) and deeper layer (D) for ROME 1, ROME 2 and ROME 3 areas. Black indicates the non-identified fraction of POC, here called “other POC”. (B) Average contribution of the hydrolysable fraction of proteins and (C) of the hydrolysable carbohydrates to the POC in the three areas. Standard deviations of POC are reported. Vertical dotted lines: UML, oblique lines: deeper layer.

Fig. 8. PCA for the entire ROME cruise and the previous studies in the upper mixed layer (UML, coloured markers) and deeper layer (DL, blue markers). Two main groups (A and B) are composed of the sub-groups a1 and a2 (A), b1 and b2 (B). The ellipses are drawn following the results of the cluster analysis on the normalised data (Euclidean distance = 1.8). See text and Table 2 for details. The vectors of the variables are reported on the upper left of the plot.

Fig. 9. Plot of the POC concentration and caloric value of the POM for the upper mixed layer (A) and the deeper layer (B). Black numbers and markers refer to the previous studies in the Ross Sea and coastal Terra Nova Bay (TNB), red numbers and markers refer to the ROME cruise results. Coloured boxes group the stations that have similar ice-related features (blue: pack-ice coverage, green: marginal ice zone – MIZ, red: polynya) or belong to the coastal sites (violet). See Table 2 for details.

722 Table 1. Position of the stations sampled for POM characterisation during the ROME cruise in 2014, depth of the

723 upper mixed layer (UML) and number of sampled depths for each station.

724

| | station | date | longitude (°E) | latitude (°S) | UML depth (m) | sampled depths |
|---|---|---|---|---|---|---|
| ROME 1 | 9 | 16 Jan | 173.87 | 75.00 | 38 | 5 |
| | 11 | 16 Jan | 172.03 | 75.00 | 29 | 5 |
| | 13 | 16 Jan | 170.76 | 75.00 | 32 | 5 |
| | 16 | 17 Jan | 169.50 | 74.83 | 15 | 5 |
| | 18 | 17 Jan | 169.51 | 74.51 | 17 | 5 |
| | 20 | 17 Jan | 169.88 | 73.99 | 14 | 5 |
| ROME 2 | 33 | 26 Jan | 166.06 | 74.70 | 18 | 4 |
| | 34 | 26 Jan | 165.75 | 74.76 | 13 | 5 |
| | 36 | 27 Jan | 165.18 | 74.88 | 12 | 5 |
| | 39 | 27 Jan | 166.06 | 74.86 | 24 | 4 |
| | 43 | 27 Jan | 164.98 | 74.79 | 14 | 4 |
| | 45 | 28 Jan | 165.49 | 74.82 | 15 | 5 |
| ROME 3 | 48 | 31 Jan | 167.83 | 76.40 | 33 | 5 |
| | 50 | 31 Jan | 168.65 | 76.40 | 36 | 5 |
| | 52 | 1 Feb | 169.53 | 76.42 | 75 | 4 |
| | 55 | 1 Feb | 168.40 | 76.43 | 44 | 5 |
| | 56 | 1 Feb | 168.16 | 76.54 | 12 | 5 |
| | 65 | 2 Feb | 169.58 | 76.50 | 115 | 4 |
| | 67 | 2 Feb | 168.72 | 76.50 | 51 | 5 |
| | 69 | 2 Feb | 168.01 | 76.50 | 14 | 4 |
| | 75 | 3 Feb | 168.80 | 76.38 | 42 | 5 |

725

Table 2. Features of the stations sampled during previous researches, here used as a comparison for the ROME cruise observations.

| area | season | environmental features | station | lat °S | long °E | reference |
|---|---|---|---|---|---|---|
| Ross Sea | spring | polynya | MP | 76.50 | 175.00 | Fabiano et al. (2000) |
| | | MIZ | 8 | 75.16 | 175.18 | |
| | | MIZ | 10 | 74.84 | 174.88 | |
| | | MIZ | 28 | 74.70 | 172.01 | |
| | | MIZ | 30 | 74.69 | 164.18 | |
| | | pack | 27 | 71.94 | 174.98 | |
| | | pack | 29 | 74.98 | 167.99 | |
| | early summer | polynya | 15 | 72.35 | 179.78 | Fabiano et al. (1993); Catalano et al. (1997) |
| | | polynya | 17 | 73.23 | 179.84 | |
| | | polynya | 19 | 74.95 | 179.82 | |
| | | polynya | 21 | 74.98 | 174.87 | |
| | | MIZ | 23 | 74.99 | 170.00 | |
| | | MIZ | 25 | 74.95 | 165.25 | |
| Terra Nova Bay | summer | coastal-open waters | TNB | 74.78 | 164.17 | Povero et al. (2001) |
| | | | TNBa | 74.75 | 164.17 | Fabiano et al. (1995) |
| | | | TNBb | 74.70 | 164.13 | Fabiano et al. (1997) |

730 Table 3. Average data and standard deviation (sd) for the upper mixed layer (UML) and the deeper layer (DL) of the ROME 1, ROME 2 and ROME 3 stations.

| position | station | water | Chl-a | | PON | | POC | | PRT | | h-PRT | | CHO | | h-CHO | | LIP | | POC/Chl-a | | POC/PON | | PRT/CHO | |
|---|---|---|---|---|---|---|---|---|---|---|---|---|---|---|---|---|---|---|---|---|---|---|---|---|
| | | layer | µg/l | sd | µg/l | sd | µg/l | sd | µg/l | sd | µg/l | sd | µg/l | sd | µg/l | sd | µg/l | sd | | sd | | sd | | sd |
| ROME 1 | 9 | UML | 1.62 | 0.06 | 48.7 | 2.1 | 297.3 | 13.7 | 319.7 | 3.9 | 84.2 | 1.1 | 96.7 | 15.0 | 7.4 | 8.8 | 80.6 | 17.2 | 184.2 | 15.3 | 6.1 | 0.0 | 3.3 | 0.5 |
| | | DL | - | - | 6.7 | 6.5 | 48.5 | 39.5 | 47.6 | 47.9 | 18.4 | 14.2 | 21.6 | 13.4 | 5.0 | 2.1 | 18.3 | 18.6 | - | - | 8.0 | 2.4 | 1.9 | 1.0 |
| | 11 | UML | 1.66 | 0.14 | 50.3 | 5.5 | 290.5 | 19.2 | 324.4 | 23.8 | 78.0 | 1.6 | 123.7 | 24.3 | - | - | - | - | 174.8 | 2.7 | 5.8 | 0.3 | 2.7 | 0.3 |
| | | DL | - | - | 5.9 | 3.5 | 39.6 | 15.6 | 49.4 | 17.4 | 17.1 | 6.6 | 16.3 | 5.9 | - | - | - | - | - | - | 7.4 | 1.6 | 3.1 | 1.2 |
| | 13 | UML | 2.02 | 0.35 | 44.9 | 15.9 | 275.1 | 98.0 | 335.3 | 116.1 | 116.1 | 65.1 | 108.5 | 52.3 | 18.3 | 21.8 | 67.7 | 22.6 | 133.7 | 25.3 | 6.1 | 0.0 | 3.2 | 0.5 |
| | | DL | - | - | 4.7 | 3.3 | 40.3 | 30.2 | 45.1 | 34.3 | 19.3 | 16.7 | 22.5 | 11.9 | 4.0 | 3.0 | 14.8 | 13.6 | - | - | 6.8 | 0.8 | 1.9 | 0.6 |
| | 16 | UML | 2.99 | 0.04 | 48.5 | 41.1 | 301.0 | 202.5 | 333.6 | 225.8 | 105.4 | 44.1 | 118.9 | 82.1 | 13.8 | 16.3 | 67.1 | 5.1 | 101.2 | 69.1 | 5.6 | 0.2 | 2.8 | 0.0 |
| | | DL | - | - | 4.3 | 2.0 | 32.3 | 19.3 | 34.1 | 34.3 | 15.9 | 15.2 | 19.1 | 6.3 | 2.6 | 1.9 | 5.6 | 4.9 | - | - | 6.6 | 0.4 | 1.5 | 1.1 |
| | 18 | UML | 1.50 | 0.22 | 38.1 | 15.8 | 208.1 | 97.3 | 240.7 | 107.4 | 69.9 | 39.1 | 63.7 | 45.3 | - | - | - | - | 144.9 | 86.2 | 5.5 | 0.2 | 4.3 | 1.3 |
| | | DL | - | - | 4.4 | 1.8 | 27.1 | 8.5 | 27.0 | 10.4 | 8.6 | 4.4 | 9.6 | 2.2 | - | - | - | - | - | - | 6.3 | 0.7 | 2.8 | 0.5 |
| | 20 | UML | 2.32 | 0.16 | 18.3 | 0.7 | 112.4 | 4.3 | 134.7 | 15.8 | 44.6 | 1.3 | 52.6 | 6.2 | 2.5 | 1.2 | 27.5 | 9.4 | 48.5 | 1.5 | 5.7 | 0.6 | 2.6 | 0.6 |
| | | DL | - | - | 2.7 | 1.7 | 21.6 | 11.4 | 15.7 | 15.3 | 5.6 | 6.1 | 12.8 | 4.1 | 1.4 | 1.5 | 9.4 | 2.8 | - | - | 7.3 | 0.3 | 1.1 | 0.8 |
| ROME 2 | 33 | UML | 1.10 | 0.04 | 34.0 | 5.7 | 192.3 | 36.7 | 226.5 | 63.8 | 76.0 | 18.6 | 87.8 | 42.1 | - | - | - | - | 174.0 | 27.2 | 5.7 | 0.2 | 2.7 | 0.6 |
| | | DL | - | - | 11.4 | 4.2 | 70.2 | 25.5 | 63.1 | 28.0 | 24.1 | 9.1 | 23.3 | 7.0 | - | - | - | - | - | - | 6.2 | 0.0 | 2.6 | 0.4 |
| | 34 | UML | 2.63 | 0.10 | 26.9 | 8.7 | 195.0 | 16.9 | 206.0 | 49.7 | 79.1 | 14.2 | 128.0 | 32.3 | 17.9 | 10.4 | 49.3 | 2.6 | 74.4 | 9.2 | 6.5 | 0.4 | 1.7 | 0.8 |
| | | DL | - | - | 18.7 | 5.9 | 145.5 | 57.1 | 136.7 | 62.6 | 54.4 | 28.0 | 98.6 | 63.0 | 16.8 | 24.4 | 22.0 | 12.9 | - | - | 7.4 | 0.7 | 1.5 | 0.4 |
| | 36 | UML | 2.18 | 0.36 | 36.1 | 2.7 | 212.9 | 20.2 | 242.1 | 2.6 | 77.5 | 6.1 | 68.6 | 3.1 | - | - | - | - | 117.5 | 64.1 | 5.9 | 0.1 | 3.5 | 0.1 |
| | | DL | - | - | 16.1 | 11.9 | 129.2 | 92.2 | 95.8 | 61.6 | 29.4 | 17.1 | 54.5 | 40.6 | - | - | - | - | - | - | 8.0 | 0.8 | 1.8 | 0.5 |
| | 39 | UML | 1.00 | 0.06 | 43.1 | 1.1 | 233.5 | 1.2 | 277.3 | 16.7 | 86.7 | 11.9 | 104.2 | 11.8 | 23.5 | 5.0 | 32.5 | 12.1 | 232.9 | - | 5.4 | 0.1 | 2.7 | - |
| | | DL | - | - | 15.2 | 9.0 | 108.3 | 74.0 | 115.3 | 79.8 | 52.5 | 30.6 | 76.3 | 61.7 | 7.9 | 6.1 | 23.2 | 18.5 | - | - | 6.7 | 1.0 | 1.6 | 0.2 |
| | 43 | UML | 1.52 | 0.12 | 38.6 | 3.6 | 233.5 | 0.4 | 306.7 | 36.8 | 97.1 | 11.8 | 102.5 | 9.2 | - | - | - | - | 153.5 | - | 6.1 | 0.6 | 3.0 | - |
| | | DL | - | - | 14.3 | 10.5 | 100.0 | 74.2 | 115.5 | 104.5 | 41.1 | 39.3 | 62.9 | 47.8 | - | - | - | - | - | - | 7.0 | 0.1 | 1.7 | 0.3 |
| | 45 | UML | 1.30 | 0.14 | 33.5 | 0.7 | 200.8 | 4.6 | 259.2 | 16.6 | 102.5 | 6.0 | 109.0 | 21.8 | 3.3 | 0.4 | 14.9 | 3.9 | 154.4 | - | 6.0 | 0.0 | 2.4 | - |
| | | DL | - | - | 24.4 | 14.7 | 162.6 | 97.5 | 174.5 | 123.5 | 64.9 | 39.6 | 111.6 | 81.4 | 8.7 | 12.2 | 16.0 | 12.2 | - | - | 6.9 | 0.6 | 1.5 | 0.5 |
| ROME 3 | 48 | UML | 3.01 | 0.16 | 46.7 | 5.3 | 248.4 | 19.3 | 304.5 | 4.9 | 84.1 | 5.7 | 69.2 | 21.2 | - | - | - | - | 82.5 | 1.9 | 5.3 | 0.2 | 4.6 | 1.3 |
| | | DL | - | - | 4.7 | 2.4 | 31.9 | 15.8 | 28.0 | 13.8 | 9.5 | 4.6 | 9.6 | 1.8 | - | - | - | - | - | - | 6.9 | 0.4 | 2.8 | 0.9 |
| | 50 | UML | 3.04 | 0.09 | 44.6 | 1.4 | 263.4 | 8.8 | 298.3 | 9.3 | 79.9 | 5.5 | 102.5 | 4.3 | 14.5 | 12.1 | 52.6 | 16.4 | 86.8 | 5.5 | 5.9 | 0.4 | 2.9 | 0.0 |
| | | DL | - | - | 8.7 | 8.5 | 62.1 | 54.6 | 72.8 | 72.2 | 34.5 | 31.2 | 24.4 | 16.5 | 2.8 | 2.2 | 17.5 | 20.5 | - | - | 7.8 | 0.9 | 2.7 | 1.3 |
| | 52 | UML | 1.09 | 0.05 | 26.2 | 5.3 | 160.9 | 11.0 | 183.6 | 22.2 | 57.5 | 3.0 | 49.1 | 7.3 | - | - | - | - | 148.1 | 3.6 | 6.3 | 1.7 | 3.8 | 0.1 |
| | | DL | - | - | 2.6 | 0.6 | 23.4 | 1.7 | 23.3 | 1.1 | 9.5 | 2.1 | 6.8 | 0.1 | - | - | - | - | - | - | 9.5 | 1.9 | 3.4 | 0.2 |
| | 55 | UML | 3.16 | 2.19 | 42.1 | 24.6 | 252.7 | 130.7 | 305.0 | 184.3 | 106.9 | 51.0 | 103.8 | 69.3 | 24.3 | 18.5 | 78.4 | 16.6 | 103.7 | 51.6 | 5.8 | 0.1 | 3.3 | 0.9 |
| | | DL | - | - | 3.6 | 0.7 | 23.8 | 1.2 | 21.0 | 2.7 | 13.6 | 0.9 | 11.9 | 0.9 | 5.1 | 0.3 | 10.5 | 1.1 | - | - | 6.0 | 0.2 | 1.8 | 0.4 |
| | 56 | UML | 2.71 | 1.92 | 45.7 | 9.8 | 245.1 | 65.7 | 332.6 | 75.2 | 91.6 | 21.0 | 64.7 | 30.3 | - | - | - | - | 109.2 | 53.1 | 5.3 | 0.3 | 5.5 | 1.4 |
| | | DL | - | - | 10.2 | 11.5 | 57.1 | 53.8 | 75.8 | 87.4 | 24.8 | 30.6 | 17.6 | 15.6 | - | - | - | - | - | - | 6.7 | 1.8 | 3.7 | 1.2 |
| | 65 | UML | 1.10 | 0.00 | 22.7 | 0.1 | 123.9 | 12.6 | 158.4 | 13.9 | 30.2 | 23.7 | 41.0 | 1.2 | - | - | - | - | 112.2 | 11.0 | 5.5 | 0.6 | 3.9 | 0.2 |
| | | DL | - | - | 5.8 | 2.8 | 34.4 | 15.5 | 42.3 | 23.6 | 15.7 | 7.9 | 12.1 | 5.0 | - | - | - | - | - | - | 6.0 | 0.2 | 3.4 | 0.6 |
| | 67 | UML | 3.64 | 0.64 | 45.1 | 14.2 | 254.6 | 77.9 | 327.0 | 79.7 | 95.9 | 11.7 | 94.3 | 42.5 | 6.3 | 5.1 | 70.0 | 26.0 | 68.8 | 10.2 | 5.7 | 0.2 | 3.8 | 1.2 |
| | | DL | - | - | 4.5 | 0.8 | 35.0 | 8.4 | 33.0 | 12.4 | 13.8 | 3.1 | 18.1 | 7.4 | 2.6 | 0.1 | 15.4 | 0.8 | - | - | 6.1 | 0.5 | 1.8 | 0.1 |
| | 69 | UML | 2.14 | 0.12 | 27.6 | 1.9 | 175.2 | 25.0 | 199.6 | 11.3 | 48.1 | 31.8 | 53.4 | 5.7 | - | - | - | - | 81.8 | 7.1 | 6.3 | 0.4 | 3.7 | 0.2 |
| | | DL | - | - | 7.9 | 6.9 | 49.5 | 32.7 | 73.1 | 58.3 | 21.6 | 14.2 | 13.6 | 8.4 | - | - | - | - | - | - | 7.3 | 2.3 | 5.0 | 1.2 |
| | 75 | UML | 4.03 | 1.02 | 51.9 | 14.3 | 286.7 | 76.2 | 366.5 | 94.0 | 90.0 | 10.8 | 85.8 | 37.0 | - | - | - | - | 70.9 | 1.3 | 5.5 | 0.1 | 4.5 | 0.9 |
| | | DL | - | - | 4.0 | 1.2 | 27.5 | 2.0 | 22.7 | 9.1 | 8.2 | 6.2 | 6.8 | 1.5 | - | - | - | - | - | - | 7.2 | 1.6 | 3.3 | 0.6 |

Chl-a: chlorophyll-a, PON: particulate organic nitrogen, POC: particulate organic carbon, PRT: particulate proteins, h-PRT: hydrolysable particulate proteins, CHO: particulate carbohydrates, h-CHO: hydrolysable particulate carbohydrates, LIP: lipids, POC/Chl: POC/chlorophyll-a ratio, PRT/CHO: protein/carbohydrate ratio, POC/PON: POC/PON ratio.

734 Table 4. Significant correlations between the different variables for each area investigated during the ROME
735 cruise. Underlined numbers: p<0.05, normal numbers: p<0.01, bold numbers: p<0.001. The number of
736 observation varied in the three Legs: in ROME 1 chlorophyll-a showed 13 observations, hydrolysable
737 carbohydrate and lipid 18, the other variables 28. In ROME 2 they were: 19, 12 and 25, respectively. In
738 ROME 3: 25, 13 and 40, respectively. Abbreviations as in Table 2.
739

| | | Chl-a | PON | POC | prt | h-PRT | CHO | h-CHO |
|---|---|---|---|---|---|---|---|---|
| ROME 1 | PON | 0.68 | | | | | | |
| | POC | 0.72 | **1.00** | | | | | |
| | prt | 0.73 | **0.99** | **1.00** | | | | |
| | h-PRT | 0.76 | **0.94** | **0.95** | **0.97** | | | |
| | CHO | 0.71 | **0.97** | **0.98** | **0.98** | **0.94** | | |
| | h-CHO | - | **0.76** | **0.75** | **0.77** | **0.83** | **0.82** | |
| | LIP | *0.63* | **0.89** | **0.92** | **0.91** | **0.90** | **0.88** | 0.65 |

| | | Chl-a | PON | POC | prt | h-PRT | CHO | h-CHO |
|---|---|---|---|---|---|---|---|---|
| ROME 2 | PON | - | | | | | | |
| | POC | - | **0.96** | | | | | |
| | prt | - | **0.97** | **0.95** | | | | |
| | h-PRT | - | **0.89** | **0.90** | **0.94** | | | |
| | CHO | 0.65 | **0.68** | **0.81** | **0.77** | **0.79** | | |
| | h-CHO | - | - | - | - | - | 0.72 | |
| | LIP | - | - | - | - | - | *0.53* | *0.63* |

| | | Chl-a | PON | POC | prt | h-PRT | CHO | h-CHO |
|---|---|---|---|---|---|---|---|---|
| ROME 3 | PON | **0.95** | | | | | | |
| | POC | **0.95** | **0.99** | | | | | |
| | prt | **0.95** | **0.99** | **0.99** | | | | |
| | h-PRT | **0.86** | **0.93** | **0.94** | **0.94** | | | |
| | CHO | **0.90** | **0.93** | **0.95** | **0.94** | **0.91** | | |
| | h-CHO | *0.64* | 0.74 | 0.74 | 0.74 | 0.72 | **0.80** | |
| | LIP | 0.68 | **0.91** | **0.91** | **0.90** | **0.90** | **0.89** | 0.68 |

740

741 Table 5. Multivariate statistical analysis (ANOSIM and SIMPER) for the two main groups A and B of the PCA
742 (Fig. 8) and the sub-groups a1-a2 and b1-b2. Mean values ± standard deviation for each group and sub-
743 group are reported (POC, PRT and CHO: µg $l^{-1}$; PRT/CHO: µg $µg^{-1}$). Abbreviations as in Table 2.

744

ANOSIM

| sub-groups | R statistic | significance % |
|---|---|---|
| A vs B | 0.847 | 0.1 |
| a1 vs a2 | 0.656 | 0.1 |
| b1 vs b2 | 0.903 | 0.1 |

745

SIMPER

| groups | variable | % | | average±sd | | average±sd |
|---|---|---|---|---|---|---|
| A vs B | PRT | 32 | A: | 281.4±62.9 | B: | 58.8±47.5 |
| | PRT/CHO | 25 | | 3.6±1.0 | | 2.1±0.9 |
| | CHO | 24 | | 90.0±32.9 | | 32.7±30.0 |
| | POC | 19 | | 242.8±55.0 | | 72.4±53.9 |
| a1 vs a2 | PRT/CHO | 41 | a1: | 4.3±0.7 | a2: | 2.9±0.4 |
| | CHO | 36 | | 63.1±15.7 | | 115.1±23.0 |
| | PRT | 14 | | 243.8±60.1 | | 316.4±43.0 |
| b1 vs b2 | CHO | 47 | b1: | 15.9±5.5 | b2: | 71.5±27.1 |
| | PRT/CHO | 22 | | 2.2±1.0 | | 1.7±0.4 |
| | POC | 17 | | 40.7±14.4 | | 145.7±36.6 |
| | PRT | 14 | | 33.2±17.1 | | 118.0±41.8 |

746

**Figure 1**

Click here to download high resolution image

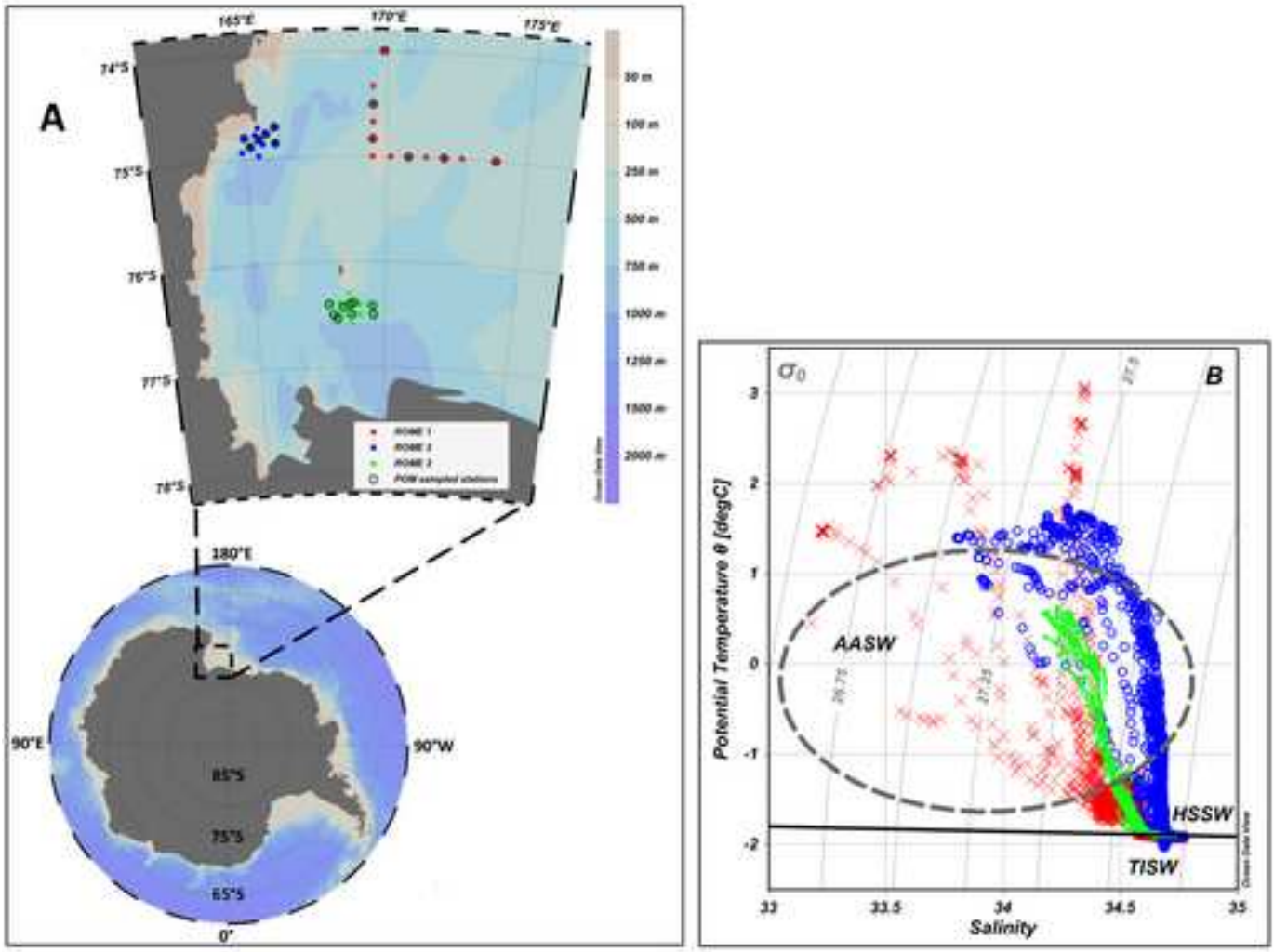

**Figure 2**

**Click here to download high resolution image**

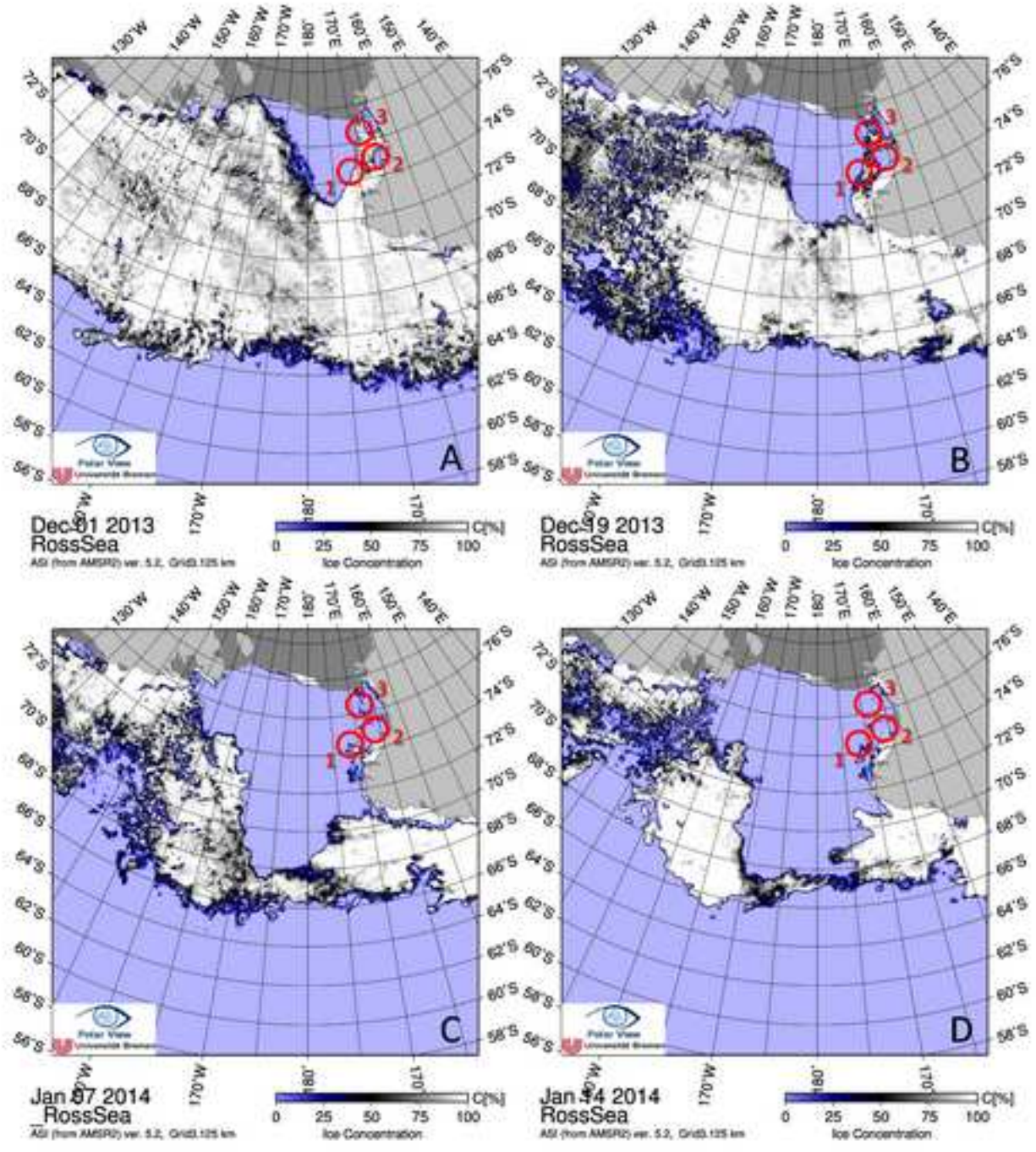

**Figure 3**

**Click here to download high resolution image**

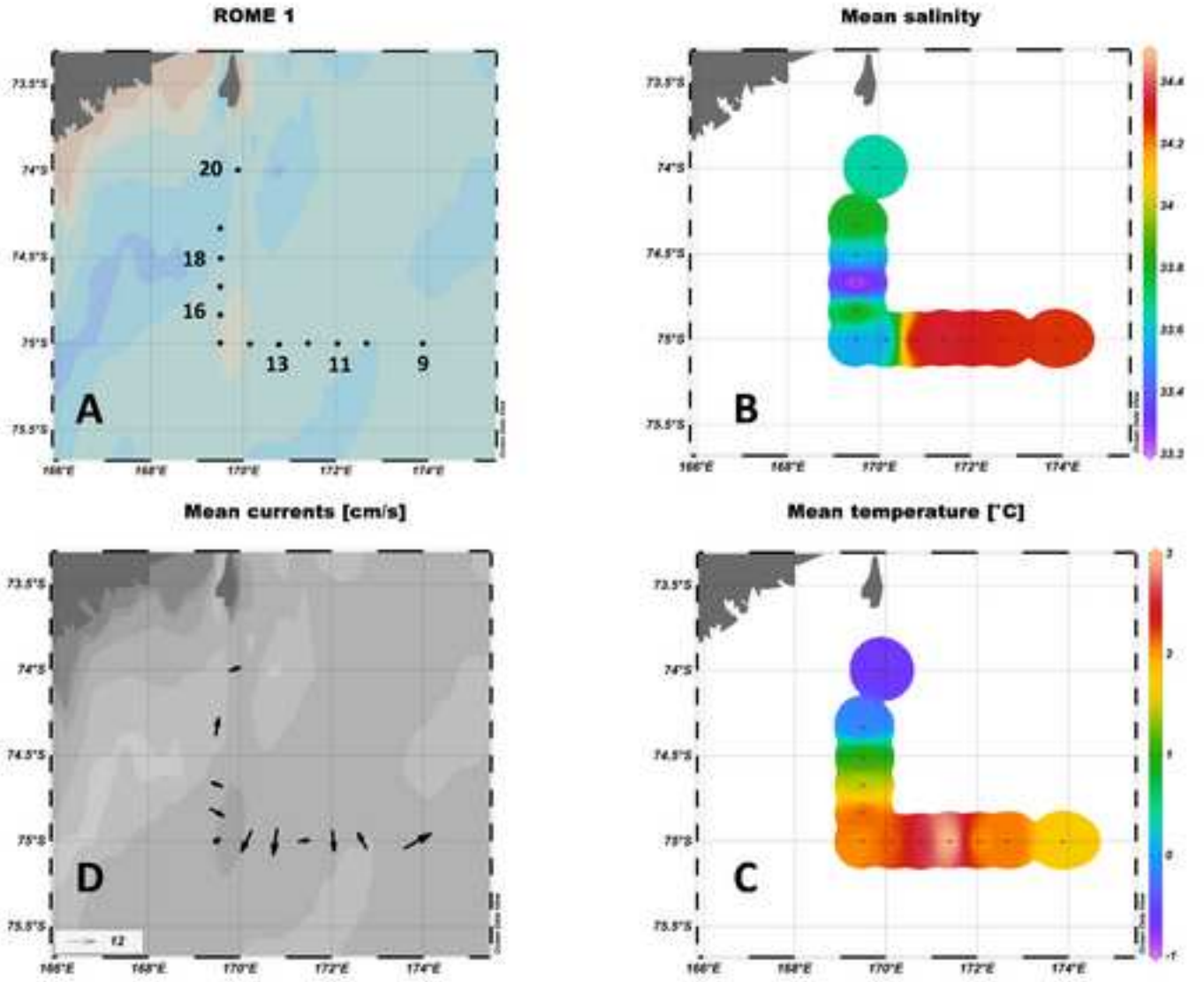

**Figure 4**

Click here to download high resolution image

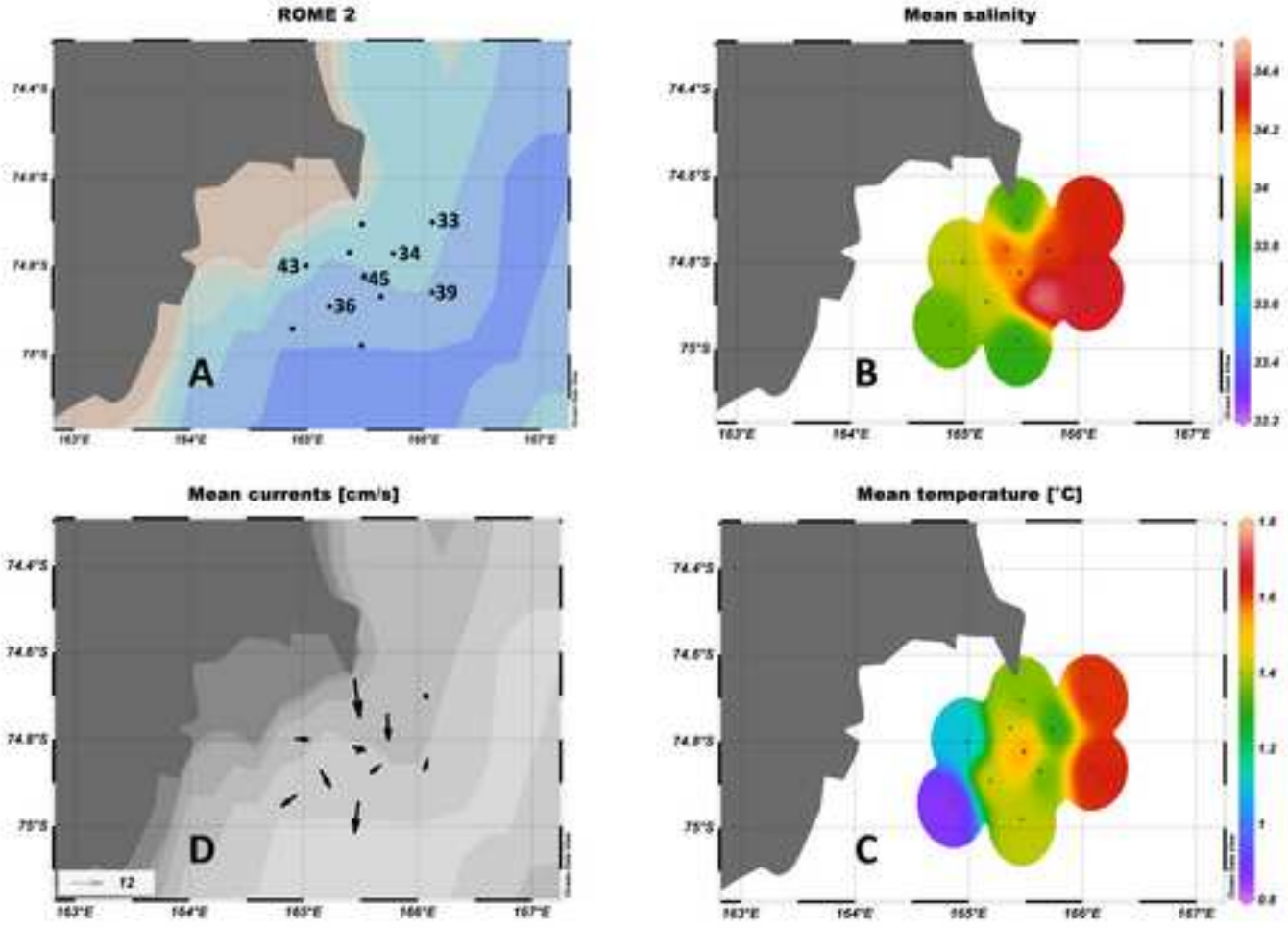

**Figure 5**

**Click here to download high resolution image**

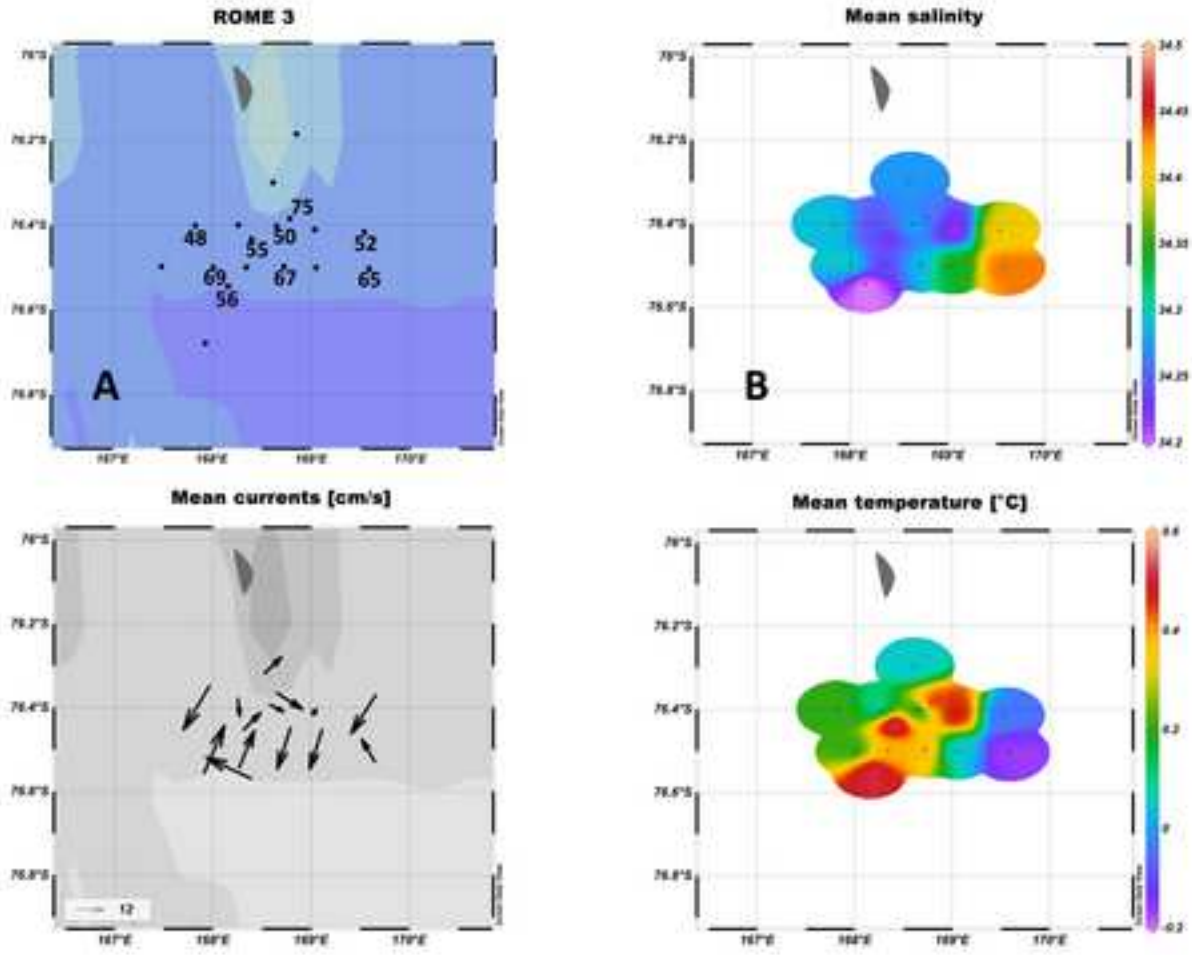

**Figure 6**

**Click here to download high resolution image**

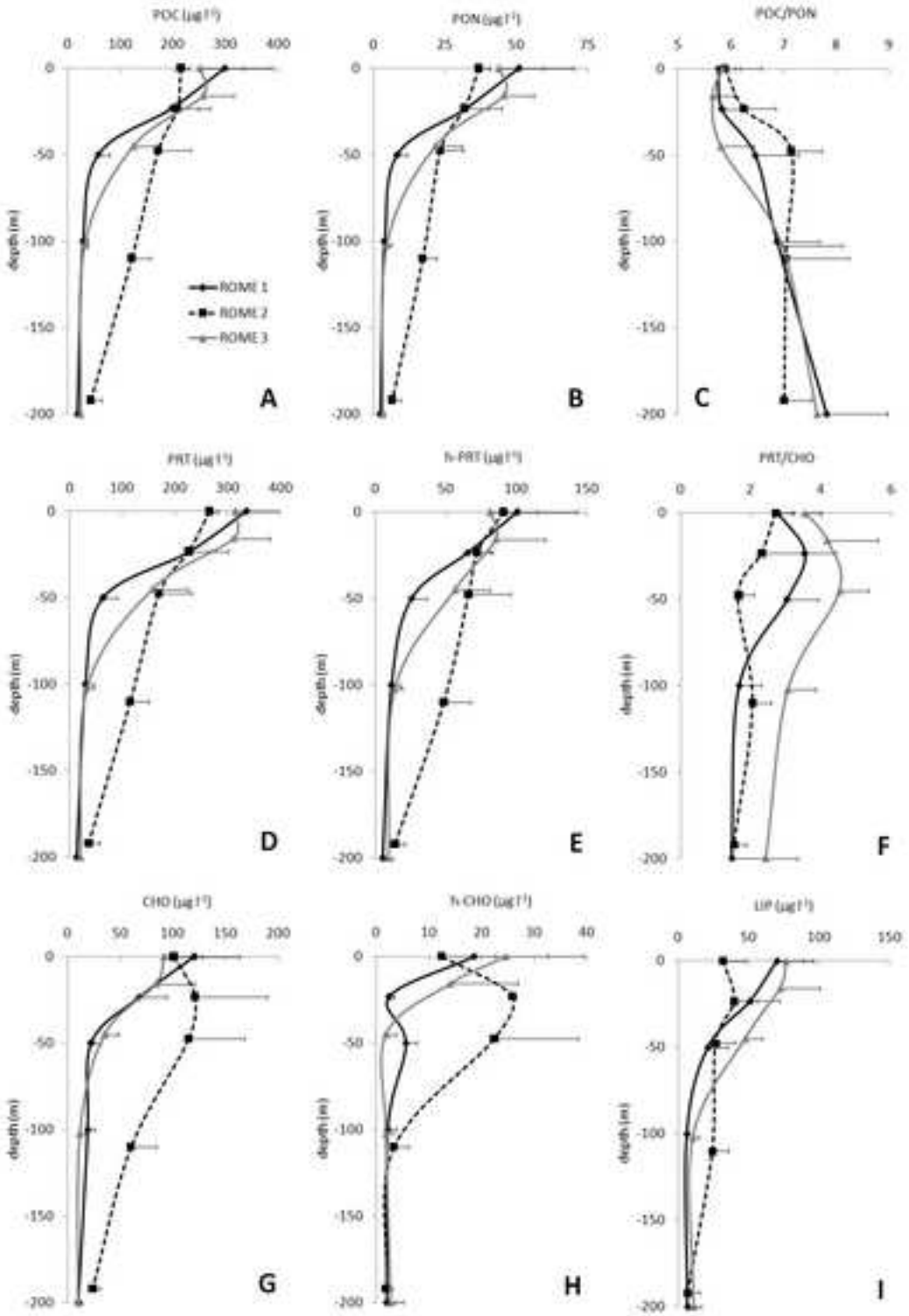

**Figure 7**

Click here to download high resolution image

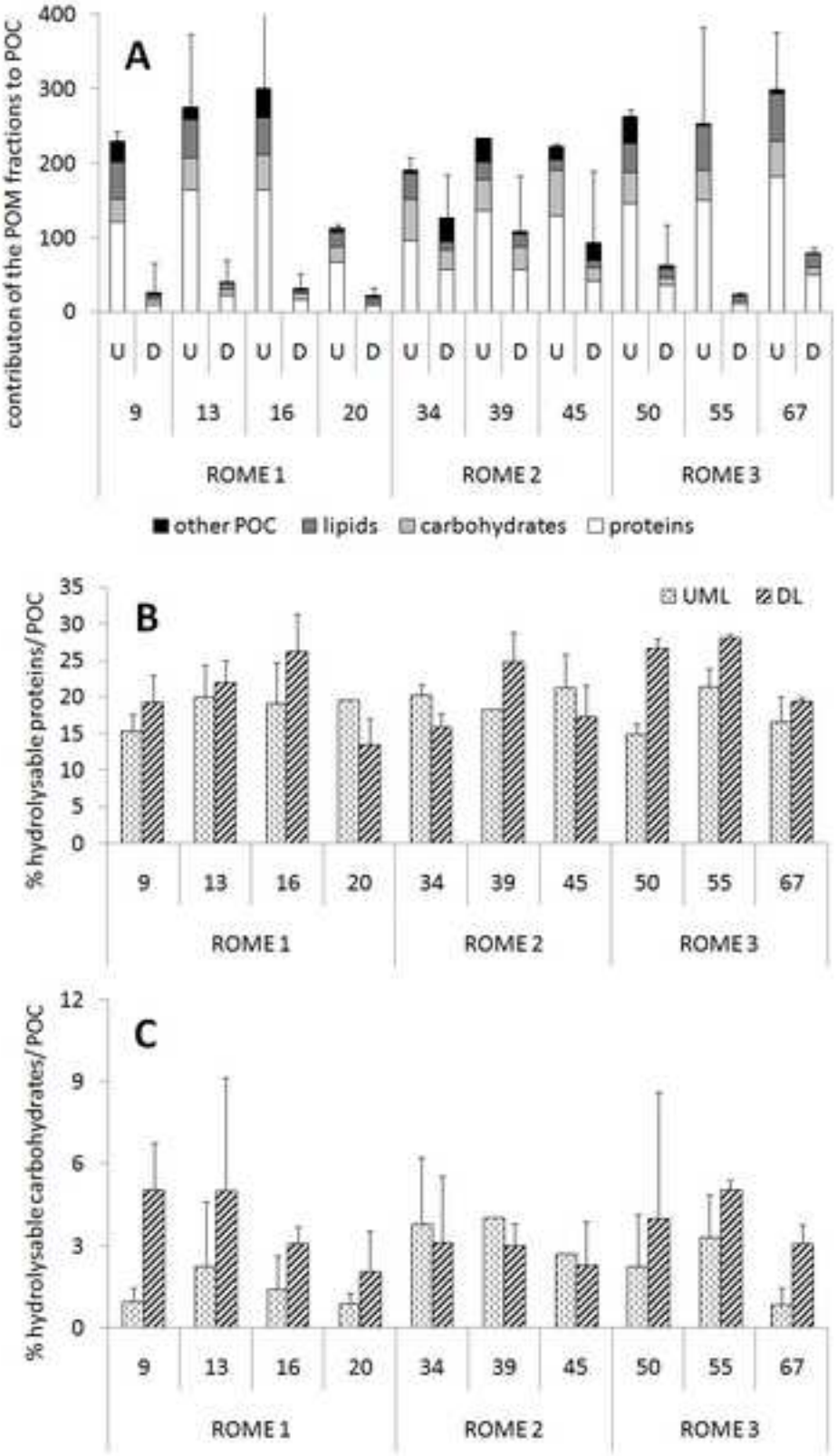

**Figure 8**

**Click here to download high resolution image**

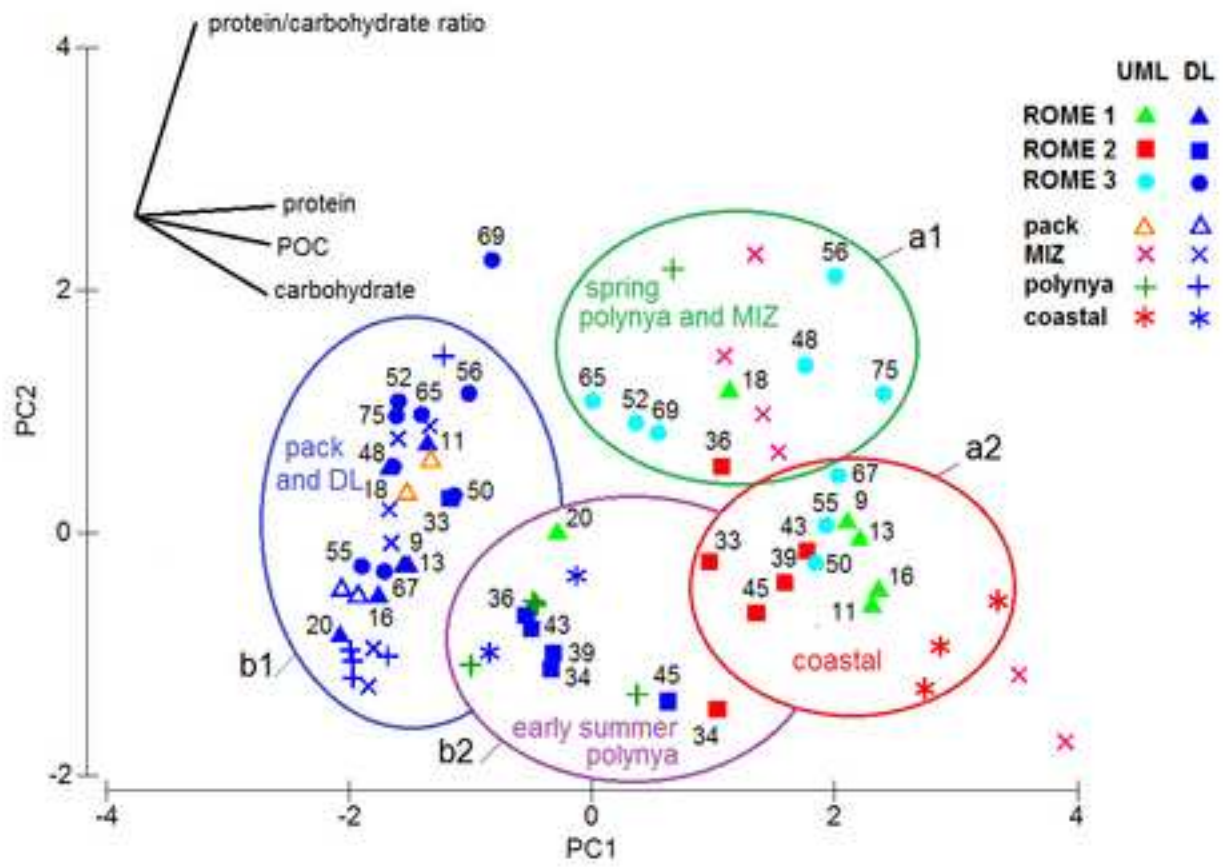

**Figure 9**

Click here to download high resolution image